Increased expression of UBE2T predicting poor survival of ovarian cancer: based on comprehensive analysis of UBE2s, clinical samples and the GEO database

Ruoyao Zou
Shengjing Hospital of China Medical University
Haoya Xu
Shengjing Hospital of China Medical University
Feifei Li
Shandong Provincial Hospital
Shengke Wang
Shengjing Hospital of China Medical University
Liancheng Zhu (medecin@126.com)
Shengjing Hospital of China Medical University https://orcid.org/0000-0002-3966-8425

Primary research

Keywords: UBE2T, UBE2s, ovarian cancer, prognostic value, bioinformatics analysis, immunohistochemistry

Posted Date: June 15th, 2020

DOI: https://doi.org/10.21203/rs.3.rs-35103/v1

Abstract

Background Ubiquitin-conjugating enzymes E2 (UBE2) have been reported in the microenvironment of various malignant tumors, but their correlation with ovarian cancer remains elusive.

Methods: The Oncomine, GEPIA, Kaplan-Meier Plotter, cBioPortal, and STRING databases were used to systematically analyze the expression pattern, prognostic value, genetic variation, and biological function of 12 members of the UBE2 gene family in ovarian cancer. UBE2T exhibited the greatest correlation with ovarian cancer and was thus further examined. Gene set enrichment analysis (GSEA), as well as analyses of function and pathway enrichment, somatic mutations, copy number variation, and methylation were performed, and the correlation with immune cell infiltration was examined to explore the mechanism underlying aberrant UBE2T expression. Finally, the expression and prognostic value of UBE2T in ovarian cancer were verified by immunohistochemical evaluation of 131 clinical ovarian samples and the Gene Expression Omnibus (GEO) database (GSE51088, GSE73614, and GSE63885 datasets) analysis.

Results: The mRNA levels of UBE2C , UBE2N , UBE2S , and UBE2T were significantly upregulated in ovarian cancer compared with those in normal ovarian tissue. In patients with ovarian serous carcinoma, UBE2A , UBE2B , UBE2C , UBE2G , and UBE2T upregulation and UBE2R2 downregulation were associated with poor overall survival. Moreover, UBE2A , UBE2N , and UBE2T upregulation and UBE2G and UBE2R2 downregulation were associated with poor progression-free survival. Immunohistochemistry revealed that UBE2T was significantly upregulated in ovarian malignant tumors compared with that in borderline tumors, benign tumors, and normal ovarian tissues, and its high expression was associated with poor prognosis. The Cox model showed that UBE2T upregulation was an independent risk factor affecting the prognosis of ovarian cancer (hazard ratio: 4.095, P= 0.029). The above results were verified in the GEO database. In addition, UBE2T was associated with specific immune cells and mainly involved in cell cycle-related events. Genomic analysis showed that TP53 and TTN mutations were associated with UBE2T expression. Gene copy number amplification and hypomethylation may be responsible for UBE2T upregulation in ovarian cancer.

Conclusions: UBE2 family members may play a role in the development of ovarian cancer. Specifically, UBE2T could serve as a new prognostic marker and therapeutic target for this disease.

Background

Ovarian cancer (OC) is the most deadly malignancy of the female reproductive system and the fifth leading cause of cancer-related death among women worldwide[1]. More than 70% of OC patients are diagnosed with advanced disease due to lack of typical clinical symptoms and effective diagnostic methods, which explains the high mortality rate of this disease. Despite major advances in surgical techniques, chemotherapy, and immunotherapy, the current treatments are still unsatisfactory, as the five-year overall survival (OS) rate is approximately 30%[2]. Hence, the identification of biomarkers with high sensitivity and specificity, as well as the comprehension of their role in OC, are urgently needed.

The tumor microenvironment consists of multiple cellular and non-cellular components that support tumor growth and suppress antitumor response. The role of this system in tumor progression and its relevance for cancer immunotherapy have been extensively demonstrated[3]. Our previous analysis of genome-wide gene expression changes in HE4-transfected OC cells showed that ubiquitination is strongly involved in the development of malignant behavior. Recent findings have also revealed that ubiquitination-related enzymes are important components of the tumor microenvironment. These enzymes include ubiquitin-activating (UBE1), ubiquitin-conjugating (UBE2), and ubiquitin-ligating (UBE3) enzymes, which facilitate ubiquitination and lead to proteasome-mediated protein degradation[4]. The *UBE2* family is composed of 40 members, which are considered as pivotal factors in the ubiquitination cascade[5]. Some studies have reported that aberrant expression of *UBE2s* in tumors has an impact on tumor prognosis, suggesting that *UBE2s* are informative tumor markers for early diagnosis and prediction of prognosis[6-8]. However, the biological role and action mechanism of these enzymes in OC have not been fully elucidated. *UBE2T*, a member of the *UBE2* family, was the first to be defined as a key factor in the Fanconi anemia pathway[9]. Several studies have confirmed that *UBE2T* plays a carcinogenic role in various types of cancer, including hepatocellular carcinoma, as well as lung, breast, stomach, bladder, and prostate cancer, but its expression level and prognostic value in OC are still unclear[10-15].

In this study, we selected 12 gene members of the *UBE2* family with a possible relationship with OC, and used bioinformatics analysis to evaluate their expression and prognostic value. *UBE2T* exhibited the greatest correlation with OC, which was verified by immunohistochemistry (IHC) and GEO database analysis. Moreover, the molecular function of *UBE2T* was explored. Our study provided valuable hints for the design of a new targeted therapy for OC.

Methods

Oncomine database analysis

Oncomine (http://www. oncomine. org) is a web-based gene chip data-mining platform consisting of microarray databases covering 19 types of human cancer. It includes 715 tumor microarrays, as well as 86,733 cancer and normal tissue samples[16]. Oncomine can be used to identify genes with differential expression in cancers and their respective normal tissues. We used Oncomine to analyze the mRNA expression of *UBE2s* in different types of cancer. The standardized normalization and parameters were as follows: *P* value <0.01, fold change >2, and gene ranking in the top 10%.

GEPIA dataset analysis

Gene Expression Profiling Interactive Analysis (GEPIA) (http://gepia.cancer-pku. cn/) is a database of RNA sequencing expression data from The Cancer Genome Atlas (TCGA) and Genotype-tissue Expression dataset (GTEx) projects, including 33 tumor types, 9,736 tumor samples, and 8,587 normal samples[17]. In this study, we used GEPIA to verify the differential expression of *UBE2s* in OC and normal ovarian tissues. In addition, the database was used to evaluate the correlations between different *UBE2* members. *P*<0.05 indicated statistically significant differences.

GEO dataset acquirement

Three distinct OC-related datasets (GSE51088, GSE73614, and GSE63885) and the corresponding clinical information were retrieved from the GEO database (https://www.ncbi.nlm.nih.gov/geo/). GSE51088, based on the GPL7264 platform (Agilent-012097 Human 1A Microarray (V2) G4110B), contained 140 epithelial ovarian malignant tumor samples, 12 borderline ovarian tumor samples, 5 benign ovarian tumor samples, and 15 normal ovarian samples[18]. GSE73614, obtained with the GPL6480 platform (Agilent-014850 Whole Human Genome Microarray 4x44K G4112F), contained 107 epithelial ovarian cancer (EOC) samples[19]. GSE63885, based on the GPL570 platform (HG-U133_Plus_2; Affymetrix Human Genome U133 Plus 2.0 Array), contained 70 serous and 5 nonserous OC samples with complete clinical data[20]. All gene expression data were subjected to log2 transformation.

TCGA data extraction and analysis

Somatic mutations data corresponding to *UBE2T* high-low expression samples were downloaded from the TCGA-OV database. Data regarding OC-related gene copy number variations were downloaded from the cBioPortal (http://www.cbioportal.org/), and the samples were divided into four groups according to the copy number as follows: single deletions, diploid normal copy, low-amplification and high-amplification. Wilcoxon test was used to compare the expression of *UBE2T* between two groups. *UBE2* genetic variations in ovarian serous cystadenocarcinoma (such as amplifications, deep deletions, fusions, and mutations) were also analyzed in the cBioPortal database. OC methylation data were obtained from the Xena browser (https://xenabrowser.net/datapages/). Pearson correlation analysis was applied to evaluate the correlation between the methylation level and the expression of *UBE2T*.

Kaplan-Meier plotter analysis

The Kaplan-Meier plotter (http://kmplot. com/analysis) contains information on 54,675 genes and 10,188 cancer samples, including breast (n=6234), lung (n=3452), ovarian (n=2190), and gastric (n=1440) cancer. This tool is used to verify the impact of biomarker genes identified from GEO, TCGA, and the Cancer Biomedical Informatics Grid project on survival [21]. In this study, the Kaplan-Meier plotter was used to evaluate the prognostic value of different *UBE2* members. OC patients were separated into a high-expression or a low-expression group, the best cutoff values were determined by algorithms embedded in KM plotter. The relevant hazard ratios (HRs), 95% confidence intervals (CIs), and log-rank *P* values were calculated.

String protein network analysis

The Search Tool for the Retrieval of Interacting Genes/Proteins (STRING) database (https://string-db. org/) is an effective tool for the analysis of functional associations between proteins. It contains information on 9.64 million proteins and 13.8 million interactions in 2,031 species[22]. We used the STRING database to predict the upstream and downstream regulatory proteins of *UBE2s* and the regulatory relations between these proteins in *Homo sapiens*. Interactions with a combined score >0.7

(high confidence) were considered significant. This information was used to construct a protein-protein interaction (PPI) network, and the Gene Ontology (GO) biological process and Kyoto Encyclopedia of Genes and Genomes (KEGG) pathway enrichment were analyzed by *ClueGO* and *CluePedia* plug-ins in Cytoscape3.2.1.

Metascape enrichment and GSEA analysis

The Metascape resource (http://metascape.org/gp/index. html) was utilized to predict the potential biological functions of target genes[23]. We used the cBioPortal database to identify genes that were co-expressed with *UBE2T*. The co-expressed genes with Spearman's correlation coefficient ≥0.35 or <−0.35 were imported into Metascape for GO and KEGG pathway enrichment analysis. In the TCGA-OV database, 379 OC cases were divided into a high- and a low-expression group according to the median expression value of *UBE2T*. GSEA 3.0 software was used to identify the potential hallmark between the two expression groups by using default weighted enrichment statistics. "h.all.v6.2.symbols.gmt" was set as gene set database, and gene permutations were set to 1000.

TISIDB immune analysis

The tumor-immune system interactions (TISIDB) database (http://cis. hku. hk/TISIDB) explores the function of genes and their role in tumor-immune interactions, and contains data on 998 genes related to antitumor immunity in 30 TCGA cancer types[24]. We employed the TISIDB database to predict correlations between *UBE2T* expression and tumor immune infiltrating cells, immune modulators, and major histocompatibility complex (MHC) molecules in OC.

Participants and specimens

A total of 131 ovarian paraffin-embedded tissue samples, surgically removed from inpatients at the Shengjing Hospital of China Medical University from 2008 to 2014, were collected. Pathological diagnosis was confirmed by two pathologists from the Department of Pathology. All patients were divided into 4 groups, including 86 cases of ovarian epithelial malignant tumors (all cases were primary OC and none of the patients received chemotherapy or hormone treatment before surgery; clinical information on all patients was complete), 20 cases of ovarian epithelial borderline tumors, 15 ovarian epithelial benign tumors, and 10 normal ovarian tissues. The median ages of patients in the above 4 groups were 53 (19-78), 44 (26-87), 46 (28-67), and 43 (32-62) years, respectively. The age differences between groups were not statistically significant (P>0.05). The study was approved by the Clinical Research Ethics Committee of Shengjing Hospital of China Medical University, and all patients signed an informed consent.

Immunohistochemistry

The rabbit anti-human polyclonal antibody against *UBE2T* (10105-2-AP, 1:75) was purchased from Proteintech (Chicago, IL, USA), and the Streptavidin-peroxidase (SP) immunohistochemistry kit was purchased from Zsbio (Beijing, China). Ovarian tissues were fixed in 10% formalin, and 5-μm thick

paraffin sections were prepared. The SP method was used to detect the expression of *UBE2T*. The presence of brownish-yellow staining on the cell membrane and in the cytoplasm was indicative of *UBE2T* positivity. A lung cancer sample was used as a positive control and phosphate-buffered saline was used instead of the antibody as a negative control. The staining intensity was classified as negative, light-yellow, brownish-yellow, and dark-brown, and scored 0, 1, 2, and 3, respectively. Based on the percentage of positive cells, the following categories were created:<5%, 5%-25%, 26%-50%, 51-75%, and >75%, which scored 0, 1, 2, 3, and 4, respectively. The final score was the product of the cell staining intensity score and the positive cell rate score: 0–2 was negative (-), 3–4 weakly positive (+), 5–8 moderately positive (++), and 9–12 strongly positive (+++). Negativity and weak positivity were considered indicative of low expression, whereas moderate and strong positivity corresponded to high expression. To minimize the errors, each tissue section was independently reviewed by two observers. Inconsistent results were reviewed by a third observer.

Statistical analysis

SPSS 22.0 software (SPSS Inc., Chicago, IL, USA) was used for statistical analysis, GraphPad Prism 8.0 (La Jolla, CA, USA) and "*survminer*" R package were employed to generate figures. *Chi* squared and Fisher's exact tests were used to analyze counting data, while Student's *t*-test was used to analyze measurement data. Kaplan-Meier survival analysis and log-rank tests of the GEO database (GSE63885 and GSE73614) were used to assess the influence of *UBE2T* on OC prognosis, and the GSE51088 dataset was used to compare the expression of *UBE2T* in different groups. Univariate and multivariate analyses were based on Cox proportional hazard regression models. *P* values <0.05 were defined as indicative of statistical significance. The patients with malignant OC were followed up, and inpatient data and telephone contacts were available. The last date of follow-up was November 30, 2019, and OS was defined as the time interval between the date of surgery and the date of death or follow-up endpoint.

Results

Expression levels of *UBE2* family members in patients with ovarian cancer

We selected 12 gene members of the *UBE2* family based on their possible association with OC, and used the Oncomine database to analyze their mRNA expression levels in different cancer and normal tissue samples (Fig. 1a and Table 1). The database contained a total of 433, 467, 450, 299, 439, 452, 409, 444, 314, 392, 299, and 443 analyses for *UBE2A*, *UBE2B*, *UBE2C*, *UBE2F*, *UBE2G*, *UBE2I*, *UBE2M*, *UBE2N*, *UBE2R2*, *UBE2S*, *UBE2T*, and *UBE2V2*, respectively. Oncomine analysis revealed that the mRNA expression of *UBE2C*, *UBE2M*, *UBE2N*, *UBE2S*, *UBE2T*, and *UBE2V2* was upregulated in patients with OC. *UBE2C* mRNA levels were significantly higher in 8 OC datasets: in Yoshihara's dataset[25], *UBE2C* was significantly upregulated in 43 cases of ovarian serous adenocarcinoma compared with that in 10 normal tissue samples (*P*=5.73E-13, fold change=12.955); in Lu's dataset[26], *UBE2C* was overexpressed in ovarian serous adenocarcinoma, endometrioid adenocarcinoma, and clear cell adenocarcinoma (*P*=1.39E-7, fold change=2.358; *P*=1.43E-4, fold change=2.298; *P*=0.001; fold change=2.156); in the TCGA,

Adib' s, and Welsh' s dataset[27, 28], *UBE2C* was highly expressed in ovarian serous carcinoma compared with that in normal tissues. (*P*=2.24E-7, fold change=10.184; *P*=0.004, fold change=3.828; *P*=8.50E-8; fold change=4.020, respectively). Similar results were reported by Bonome et al. in ovarian carcinoma (*P*=2.50E-10, fold change=4.182)[29]. Moreover, in Bonome's dataset[29], *UBE2M* (*P*=1.63E-7, fold change=2.479), *UBE2N* (*P*=6.86E-10, fold change=2.111), and *UBE2S* (*P*=5.22E-11, fold change=3.855) were upregulated in OC. In the TCGA dataset, *UBE2S* (*P*=1.53E-5, fold change=3.267) and *UBE2V2* (*P*=7.04E-8, fold change=2.031) were upregulated in ovarian serous cystadenocarcinoma. Significant *UBE2T* overexpression compared with that in normal tissues was found in Yoshihara's dataset (ovarian serous adenocarcinoma; *P*=4.30E-8, fold change=8.877)[25], and in Lu's dataset (ovarian serous adenocarcinoma and endometrioid adenocarcinoma; *P*=3.64E-8, fold change=2.751 and *P*=2.19E-6, fold change=2.814, respectively)[26] In addition, the mRNA levels of *UBE2B*, *UBE2G*, and *UBE2I* were reduced in patients with OC. In Bonome's dataset[29], *UBE2B* (*P*=2.98E-9, fold change=−2.405), *UBE2G* (*P*=6.86E-10, fold change=−2.111), and *UBE2I* (*P*=8.72E-8, fold change=−3.355) were downregulated in ovarian carcinoma compared with those in ovarian surface epithelium. A similar trend was found for *UBE2I* in Welsh's [28] and TCGA datasets: the mRNA levels of *UBE2I* in ovarian serous surface papillary carcinoma (*P*=8.10E-5, fold change=−3.672) and ovarian serous cystadenocarcinoma (*P*=2.93E-7, fold change=−2.884) were significantly lower than those in normal tissues. Moreover, Oncomine analysis showed that the mRNA expression of *UBE2A*, *UBE2F*, and *UBE2R2* was not significantly different between OC and normal tissues.

Next, we used the GEPIA database to compare the mRNA levels of different *UBE2s* in OC and normal ovarian tissues (Fig. 1b). The results indicated that the expression levels of *UBE2C*, *UBE2F*, *UBE2N*, *UBE2S*, and *UBE2T* were significantly higher in OC tissues than in normal ovarian tissues, whereas those of *UBE2A*, UBE2B, *UBE2G*, *UBE2I*, *UBE2M*, *UBE2R2*, and *UBE2V2* were not significantly different between the two groups. Combined analysis of the GEPIA and Oncomine databases revealed that the expression of *UBE2C*, *UBE2N*, *UBE2S*, and *UBE2T* was upregulated in OC compared with that in normal tissues.

Table 1 *UBE2* expression in different types of ovarian cancer and normal ovarian tissues (Oncomine)

Gene	Dataset	Tumor (cases)	Normal (cases)	Fold change	t-test	*P*-value
UBE2B	Bonome	Ovarian Carcinoma (185)	Ovarian Surface Epithelium (10)	-2.405	-14.212	2.98E-9
UBE2C	Yoshihara	Ovarian Serous Adenocarcinoma (43)	Peritoneum (10)	12.955	14.201	5.73E-13
	Lu	Ovarian Serous Adenocarcinoma (20)	Ovarian Surface Epithelium (5)	2.358	8.107	1.39E-7
	Lu	Ovarian Endometrioid Adenocarcinoma (9)	Ovarian Surface Epithelium (5)	2.298	5.260	1.43E-4
	Lu	Ovarian Clear Cell Adenocarcinoma (7)	Ovarian Surface Epithelium (5)	2.156	4.314	0.001
	TCGA	Ovarian Serous Cystadenocarcinoma (586)	Ovary (8)	10.184	16.188	2.24E-7
	Adib	Ovarian Serous Adenocarcinoma (6)	Ovary (4)	3.828	4.280	0.004
	Welsh	Ovarian Serous Surface Papillary Carcinoma (28)	Ovary (4)	4.020	13.503	8.50E-8
	Bonome	Ovarian Carcinoma (185)	Ovarian Surface Epithelium (10)	4.182	15.168	2.50E-10
UBE2G	Bonome	Ovarian Carcinoma (185)	Ovarian Surface Epithelium (10)	-2.410	-14.317	6.69E-11
UBE2I	TCGA	Ovarian Serous Cystadenocarcinoma (586)	Ovary (8)	-2.884	-12.936	2.93E-7
	Welsh	Ovarian Serous Surface Papillary Carcinoma (28)	Ovary (4)	-3.672	-4.312	8.10E-5
	Bonome	Ovarian Carcinoma (185)	Ovarian Surface Epithelium (10)	-3.355	-12.246	8.72E-8
UBE2M	Bonome	Ovarian Carcinoma (185)	Ovarian Surface Epithelium (10)	2.479	9.829	1.63E-7
UBE2N	Bonome	Ovarian Carcinoma (185)	Ovarian Surface Epithelium (10)	2.111	12.184	6.86E-10
UBE2S	Bonome	Ovarian Carcinoma (185)	Ovarian Surface Epithelium (10)	3.855	14.375	5.22E-11
	TCGA	Ovarian Serous Cystadenocarcinoma (586)	Ovary (8)	3.267	8.944	1.53E-5
UBE2T	Lu	Ovarian Endometrioid Adenocarcinoma (9)	Ovarian Surface Epithelium (5)	2.814	8.153	2.19E-6
	Lu	Ovarian Serous Adenocarcinoma (20)	Ovarian Surface Epithelium (5)	2.751	7.789	3.64E-8
	Yoshihara	Ovarian Serous Adenocarcinoma (43)	Peritoneum (10)	8.877	10.048	4.30E-8
UBE2V2	TCGA	Ovarian Serous Cystadenocarcinoma (586)	Ovary (8)	2.031	14.981	7.04E-8

Genetic alterations of *UBE2* family members in patients with OC

Genetic alterations of *UBE2* members were analyzed by using the cBioPortal database. A total of 1680 cases from three datasets (489 cases from TCGA, Nature 2011; 585 cases from TCGA, PanCancer Atlas; and 606 cases from TCGA, Provisional) of ovarian serous cystadenocarcinoma were analyzed (Fig. 2a,b). The alteration rates were 28.47%, 19.86%, and 13.5%, in the 3 OC datasets, respectively. Twelve *UBE2* genes showed various levels of genetic alteration. In all three datasets, only gene amplification was observed for *UBE2C* and *UBE2V2*; *UBE2C* exhibited the highest rate of amplification (6.35% in TCGA), while the rate of *UBE2V2* amplification was 4.46% in TCGA. Most genetic variations in *UBE2* family genes were amplifications and deep deletions, while mutations were found in *UBE2A* (0.17% in TCGA), *UBE2M* (0.17% in TCGA and TCGA pub), and *UBE2T* (0.17% in TCGA PanCan), and multiple alterations were found in *UBE2A* and *UBE2I* (both 0.17% in TCGA PanCan). In addition to gene amplification and deep deletions, *UBE2G* variations included gene fusions (1.37% in TCGA). The Kaplan-Meier curve indicated that there was no significant difference in OS and disease-free survival (DFS) regardless of the presence of alterations in one of the query genes (*P* values, 0.804 and 0.393, respectively, Fig. 2c,d)

Prognostic value of *UBE2* genes in patients with ovarian cancer

Kaplan-Meier plotter analysis was applied to assess the relationship between the mRNA expression of individual *UBE2* members and progression-free survival (PFS) in 1436 clinical OC patients (Fig. 3). We found that the mRNA levels of *UBE2A*, *UBE2B*, *UBE2C*, *UBE2G*, *UBE2N*, *UBE2R2*, and *UBE2T* were associated with OC prognosis, while those of the remaining members were not. Increased mRNA levels of *UBE2A*, *UBE2B*, *UBE2C*, *UBE2N*, and *UBE2T*, and decreased mRNA levels of *UBE2G* and *UBE2R2* were significantly associated with poor prognosis.

Ovarian serous tumors represent the most common histological subtype among ovarian tumors. The prognostic value of *UBE2* genes with expression levels significantly correlated with OC prognosis was further investigated in ovarian serous tumors. Increased mRNA levels of *UBE2A* (Fig. 4a), *UBE2B* (Fig. 4b), *UBE2C* (Fig. 4c), *UBE2G* (Fig. 4d), and *UBE2T* (Fig. 4g) were significantly correlated with poor OS in patients with ovarian serous tumors. Interestingly, increased expression of *UBE2A* (Fig. 5a) and *UBE2G* (Fig. 5d) was associated with shorter OS but longer PFS. Moreover, *UBE2N* (Fig. 5e) and *UBE2T* (Fig. 5g) upregulation was significantly correlated with poor PFS in patients with ovarian serous tumors, while *UBE2R2* downregulation (Fig. 4f, 5f) was correlated with poor OS and PFS. Based on the above results, in patients with ovarian serous tumors, the expression levels of *UBE2R2* and *UBE2T* were predictors of favorable and poor prognosis, respectively.

By integrating the results of Oncomine, GEPIA, and KM plotter, we observed that *UBE2T* was significantly upregulated in ovarian cancer compared to normal tissues, and that high *UBE2T* mRNA expression was significantly correlated with shorter OS and PFS in patients with ovarian serous tumors. Moreover, we assessed the prognostic value of *UBE2T* in relation to the pathological grade, FIGO stage, and *TP53* status of ovarian serous tumors. Increased expression of *UBE2T* was correlated with poor OS in patients with tumors of all FIGO stages ($P<0.05$, Fig. 6c,d). Moreover, *UBE2T* upregulation predicted poor OS in patients with both mutated and wild-type *TP53* ($P<0.05$, Fig. 6e,f). Although among patients with well/moderate and poor differentiation, those with high *UBE2T* expression tended to have shorter OS compared to patients with low *UBE2T* expression, the difference was not statistically significant ($P>0.05$, Fig. 6a,b).

Analysis of the interactions between *UBE2* family members

Spearman's correlation coefficients were calculated by using the GEPIA platform to investigate the relationships between the expression levels of different *UBE2* members in OC (Fig. 6g). The coefficients ranged from 0.013 (*UBE2B* vs. *UBE2M*) to 0.67 (*UBE2C* vs. *UBE2S*). The results indicated a moderate positive correlation between the expression levels of *UBE2A*, *UBE2N*, *UBE2S*, *UBE2T*, and *UBE2V2* ($0.3<r\leq0.7$), and a low positive correlation between the expression levels of *UBE2C*, *UBE2F*, *UBE2M*, and *UBE2R2* ($0<r\leq0.3$). However, *UBE2B* showed a weakly positive correlation with other *UBE2* genes, in addition to a weakly negative correlation with *UBE2C* ($r=-0.017$).

A protein-protein interaction (PPI) network consisting of 12 *UBE2* family members and 20 *UBE2*-interacting proteins was visualized by using Cytoscape (PPI enrichment *P* value <1.0E−16). Among 32 nodes, the most significant 10 proteins were *UBA2*, *UBC*, *NEDD8*, *RAD18*, *SUMO1/2*, *RANBP2*, *RABGAP1*, *ANAPC11*, and *CDC20*. Biological process analysis showed that *UBE2* proteins were mainly involved in anaphase-promoting complex-dependent catabolic processes, protein neddylation, protein sumoylation, postreplication repair, and positive regulation of ubiquitin protein ligase activity (Fig. 6h). Pathway analysis showed that the *UBE2* enzymes were mainly implicated in ubiquitin-mediated proteolysis, cell cycle, oocyte meiosis, and progesterone-mediated oocyte maturation (Fig. 6i, Additional file 1).

Molecular mechanisms related to *UBE2T* expression in ovarian cancer

A total of 536 genes were obtained from the cBioPortal database, based on Spearman's correlation coefficients higher than 0.35 between their expression and that of *UBE2T*. Information about the co-expressed genes is shown in Additional file 2. The Metascape portal was used, and $P<0.01$ was set as the threshold value to screen the top GO annotations and KEGG pathway results regarding *UBE2T* and its interactors. The top 20 GO enrichment items were classified into three functional groups: biological process (BP, 13 items), molecular function (MF, 1 items), and cellular component (CC, 6 items) (Fig. 7a). Regarding the BP, the genes co-expressed with *UBE2T* were mainly involved in cell division, cell cycle phase transition, DNA replication, DNA repair, and DNA conformation changes. Based on the MF, the identified genes were mainly associated with catalytic activity, acting on DNA. In terms of CC, the genes were enriched in the following categories: chromosomal region, nuclear chromosome, spindle, microtubule organizing center, and replication fork. The top 14 KEGG pathways for genes that were co-expressed with *UBE2T* are shown in Fig. 7b. Among these, cell cycle signaling, DNA replication, spliceosome, Fanconi anemia, and p53 signaling pathways were found to be involved in OC tumorigenesis and progression. To further determine the relationship between the enriched terms, a similarity network was constructed, where terms with a similarity >0.3 were connected by edges. The network was visualized by using Cytoscape. Each node represented an enriched term and was colored according to its cluster (Fig. 7c), and *P*-value (Fig. 7d). In patients with high *UBE2T* expression, significantly upregulated gene sets with nominal $P<0.05$ and FDR<0.25 included "HALLMARK_E2F_TARGETS" and "HALLMARK_G2M_ CHECKPOINT". The enrichment plots are shown in Fig. 7e.

The presence of somatic mutations was investigated in cases with high and low *UBE2T* expression. *TP53* and *TTN* were the top two mutated genes in both groups, and a high frequency of mutations in *DST*, *CSMD1*, *MUC17*, and *NEB* genes was specifically found in patients with high *UBE2T* expression. Moreover, mutations in *TOP2A*, *VPS13B*, *NF1*, *AHNAK*, and *FLG2* were significantly enriched in patients with low *UBE2T* expression (Fig. 7f,g). KEGG pathway analysis further demonstrated that in patients with high *UBE2T* expression the mutations mainly affected focal adhesion, calcium signaling, and ECM-receptor interactions (Fig. 7h). To explore the cause of *UBE2T* upregulation in OC, we analyzed its correlation with gene copy number and methylation level. We found that *UBE2T* expression increased with the copy number. Therefore, the high level of *UBE2T* could be partially attributed to gene amplification (Fig. 7i). The expression of *UBE2T* was negatively correlated with the methylation level, as hypomethylation was associated with high *UBE2T* expression (Pearson' s (372)=-0.125, $P=0.0162$, Fig. 7j).

Correlation between immune factors and *UBE2T* expression in ovarian cancer

Recently, immunotherapy has received increasing attention, becoming a new treatment strategy for ovarian cancer. We further explored the correlation between immune factors, including tumor-infiltrating lymphocytes (TILs) and immune modulators, and *UBE2T* expression in OC by using the TISIDB database. Immune modulators can be further classified into immune inhibitors, immune stimulators, and MHC molecules. TILs with the highest correlation with *UBE2T* expression included act_CD4 cells (Spearman: rho=0.331, $P=3.57e-09$), eosinophils (Spearman: rho=-0.424, $P<2.2E-16$), neutrophils (Spearman:

rho=-0.274, *P*=1.23E-06), and memory B cells (Spearman: rho=-0.271, *P*=1.61E-06) (Fig. 8b). Immune inhibitors with the highest correlation with *UBE2T* expression included *CSF1R* (Spearman: rho=-0.345, *P*=6.53E-10), *TGFB1* (Spearman: rho=-0.257, *P*=5.53E-06), *KDR* (Spearman: rho=-0.228, *P*=5.95E-05), and *CD160* (Spearman: rho=-0.155, *P*=0.0064) (Fig. 8d). Immune stimulators with the strongest correlation with *UBE2T* expression included *C10orf54* (Spearman: rho=-0.336, *P*=1.87E-09), *NTSE* (Spearman: rho=-0.308, *P*=4.13E-08), *TNFSF14* (Spearman: rho=-0.298, *P*=1.23E-07), and *TNFSF15* (Spearman: rho=-0.257, *P*=5.37E-06) (Fig. 8f). MHC molecules most strongly correlated with *UBE2T* expression included HLA-E (Spearman: rho=-0.173, *P*=0.00245), HLA-DOA (Spearman: rho=-0.171, *P*=0.00265), HLA-DQB1 (Spearman: rho=-0.129, *P*=0.0236), and HLA-DQA1 (Spearman: rho=-0.121, *P*=0.0341) (Fig. 8h). Therefore, *UBE2T* may affect the immune activity in the OC microenvironment by regulating the above immune factors.

UBE2T expression in different ovarian tissues

IHC staining demonstrated that *UBE2T* was mainly localized in the cytoplasm and the plasma membrane. The rates of positive and highly positive expression of *UBE2T* in ovarian epithelial malignant tumors (89.53% and 72.09%, respectively) were significantly higher than in ovarian epithelial borderline tumors (55.00% and 25.00%, respectively), ovarian epithelial benign tumors (26.37% and 13.34%, respectively), and normal ovarian tissues (20.00% and 10.00%, respectively, Fig. 9b,c). Consistently, GSE51088 analysis results showed a significant upregulation of *UBE2T* in malignant tumors compared to borderline tumors, benign tumors, and normal ovary (Fig. 9d).

Relationship between *UBE2T* expression and clinicopathological features of epithelial ovarian cancer

According to the median expression value of *UBE2T*, OC patients in GSE datasets were divided into a high-expression and a low-expression group. We found a significantly higher expression of *UBE2T* in FIGO stage III–IV patients than in FIGO stage I–II patients in both clinical samples (85.11% vs. 56.41 %, *P*=0.003) and GSE73614 (61.02% vs. 37.50 %, *P*=0.016). However, although *UBE2T* expression did not significantly correlate with age, stage of differentiation, presence of lymph node metastasis or pathologic subtype in our clinical samples, it was strongly associated with the pathological subtype of OC in GSE73614 (*P*=0.001, Table 2, 3). *UBE2T* displayed the highest high positive rate in serous carcinoma (100%) and the lowest high positive rate in clear cell carcinoma (27.03%).

Table 2 Correlation between *UBE2T* expression and clinicopathological features in ovarian cancer clinical samples

Characteristics	Cases (n=86)	Low −	+	High ++	+++	High positive rate (%)	Chi square Value (*P* value)
Age (years)							0.031 (0.861)
60	67	9	10	26	22	71.64	
≥60	19	0	5	7	7	73.68	
FIGO Stage							8.724 (0.003*)
I-II	39	7	10	11	11	56.41	
III-IV	47	2	5	22	18	85.11	
Differentiation							1.939 (0.164)
Well-moderately	47	7	9	21	10	65.96	
Poorly-undifferentiated	39	2	6	12	19	79.48	
Lymph node metastasis							1.418 (0.492)
No	57	6	12	19	20	68.42	
Yes	22	2	2	10	8	81.82	
No lymphadenectomy	7	1	1	4	1	71.43	
Pathological subtype							7.963 (0.093)
Mucinous	6	2	2	2	0	33.33	
Endometrioid	7	1	2	3	1	57.14	
Serous	57	5	10	23	19	73.68	
Poorly differentiated adenocarcinoma	10	1	1	3	5	80.00	
Clear cell carcinoma	6	0	0	2	4	100.00	

Table 3 Correlation between *UBE2T* expression and clinicopathological features in ovarian cancer patients of the GSE73614 dataset

Characteristics	Cases (n=107)	UBE2T expression		High positive rate (%)	Chi square Value (*P* value)
		Low	High		
Age (years)					0.231 (0.631)
60	52	27	25	48.08	
≥60	55	26	29	52.73	
FIGO Stage					5.856 (0.016*)
I-II	48	30	18	37.50	
III-IV	59	23	36	61.02	
Differentiation					3.645 (0.162)
Moderately	29	17	12	41.37	
Poorly	69	34	35	50.72	
Undifferentiated	9	2	7	77.78	
Pathological subtype					14.772 (0.001*)
Clear cell carcinoma	37	27	10	27.03	
Endometrioid	66	26	40	60.61	
Serous	4	0	4	100	

Relationship between *UBE2T* expression and prognosis in patients with epithelial ovarian cancer

During the follow-up period, of 86 patients with epithelial ovarian cancer, 32 died (37.20%) and 12 were lost to follow-up (13.95%). The 5-year OS rate was 69.7% and the mean survival time 89.7 months (95% confidence interval (CI): 80.6 98.8 months). Kaplan-Meier survival analysis revealed that in patients with high *UBE2T* expression the mean OS was significantly lower than that in those with low *UBE2T* expression (*P*=0.00093, Fig. 9e). Univariate Cox regression analysis indicated that the OS of OC patients was markedly correlated with *UBE2T* expression, FIGO stage, and differentiation status (HR 6.462, 4.029, and 0.372, respectively, all *P*<0.05). Multivariate analysis showed that high *UBE2T* expression, advanced stage, and poorly differentiated or undifferentiated status were independent risk factors in patients with OC (HR: 4.095, 3.210, and 0.422, respectively, all *P*<0.05, Table 4). Furthermore, high *UBE2T* expression was confirmed to be a predictor of poor OS in the GSE73614 (*P*=0.035, Fig. 9f) and GSE63885 (*P*=0.03,

Fig. 9g) datasets. Moreover, application of the Cox regression model to the GSE63885 dataset confirmed high *UBE2T* expression as an independent risk factor for OS in OC patients (HR=1.717, *P*=0.031, Table 5).

Table 4 Univariate and multivariate analyses of overall survival in ovarian cancer clinical samples

Variable	Univariate analysis HR (95% CI)	*P* value	Multivariate analysis HR (95% CI)	*P* value
Age				
60 vs. ≥60	1.345 (0.604-2.995)	0.469		
UBE2T expression				
High vs. low	6.462 (1.875-22.266)	0.003	4.095 (1.154-14.533)	0.029
FIGO Stage				
I-II vs. III-IV	4.029 (1.733-9.367)	0.001	3.210 (1.348-7.640)	0.008
Differentiation				
Poorly-undifferentiated vs. well-moderately	0.372 (0.179-0.772)	0.008	0.422 (0.201-0.884)	0.022
Pathological subtype				
Serous vs. nonserous	1.177 (0.575-2.409)	0.656		
Lymph node metastasis				
Yes vs. no	1.964 (0.959-4.022)	0.065		

Table 5 Univariate and multivariate analyses of overall survival in ovarian cancer patients of the GSE63885 dataset

Variable	Univariate analysis HR (95% CI)	*P* value	Multivariate analysis HR (95% CI)	*P* value
UBE2T expression				
High vs. low	1.711 (1.048-2.793)	0.032	1.717 (1.052-2.803)	0.031
FIGO Stage				
II-III vs. IV	2.214 (1.093-4.485)	0.027	2.226 (1.102-4.495)	0.026
Differentiation				
Poorly-undifferentiated vs. moderately	2.321 (1.040-5.178)	0.04		
Pathological subtype	1.293 (0.517-3.233)	0.582		
Serous vs. nonserous				

Discussion

E2-conjugating enzymes play a central role in the formation and progression of various tumors[30]. Although the role of some *UBE2* members in OC has been confirmed, to our knowledge, no studies have comprehensively analyzed the prognostic value and functional mechanism of the *UBE2* family in OC. In this study, a systematic bioinformatics analysis was conducted to evaluate the potential role of *UBE2* family genes as biomarkers of OC.

UBE2A and *UBE2B* are two *RAD6* homologs originally identified in yeast and required for DNA repair[31]. They are both upregulated in OC compared to normal ovarian tissues, and their high expression is associated with poor prognosis in OC patients[6]. Downregulation of *RAD6* was previously found to reduce the expression of the cancer stem cell markers, *ALDH1A1* and *SOX2*, and to increase the sensitivity of OC cells to carboplatin[32]. *UBE2C* is a key regulator of cell cycle progression and mitosis[33]. It is highly expressed in epithelial ovarian cancer (EOC), especially in high-grade serous adenocarcinoma, and its high expression is an independent risk factor affecting the prognosis of EOC patients[34]. Another study showed that blocking *UBE2C* expression by RNA interference inhibits the growth of OC cell lines[35]. Two neddylation conjugating E2 enzymes, *UBE2M* and *UBE2F*, were found to play essential

roles in paclitaxel (PTX)-induced cytotoxicity and tubulin polymerization in OC cell lines. A recent study reported that *UBE2M* and *UBE2F* knockdown impairs protein neddylation and reduces the antitumor activity of PTX in OC, suggesting new research directions on PTX chemoresistance [36]. The results of our bioinformatics analyses were consistent with previous reports. Kaplan-Meier plotter analysis showed that increased *UBE2A* and *UBE2B* expression was associated with poor PFS in OC patients and poor OS in patients with serous ovarian cancer. *UBE2C* expression was significantly higher in OC compared to normal tissues, and predicted poor prognosis. Although *UBE2F* and *UBE2M* were significantly more expressed in OC compared to normal tissues, their levels had no correlation with prognosis.

UBE2I and *UBE2N* are involved in DNA repair and cell apoptosis[37, 38]. *UBE2I* expression was higher in OC than in normal tissues, and correlated with clinicopathologic parameters. Moreover, *UBE2I* expression level was higher in ovarian serous carcinoma compared to ovarian myxoid carcinoma, endometrioid carcinoma, and clear cell carcinoma, and in advanced or poorly differentiated EOC compared to early or well-differentiated EOC. Guo et al. reached similar conclusions, suggesting that *UBE2I* may be involved in the progression and histopathological differentiation of OC[39, 40]. The downregulation of *UBE2N* in OC may be related to the acquisition of resistance to PTX through the DNMT1-CHFR-Aurora A pathway. Thus, *UBE2N* is a potential target of drugs aiming at reversing PTX resistance in patients with OC[41]. *UBE2R2* plays a role in the ubiquitin-proteasome pathway[42], and the combination of UBE2R2-SMYD3-p53 significantly promotes p53 ubiquitination and degradation, thereby inducing EOC progression and metastasis[43]. However, some of our data were inconsistent with previous results. Oncomine analysis showed that *UBE2I* and *UBE2N* were significantly downregulated and upregulated in OC, respectively. *UBE2N* overexpression was associated with poor PFS in OC patients, while *UBE2R2* downregulation correlated with poor OS and PFS in patients with ovarian serous tumors. We attribute these contradictory findings to background heterogeneity between different databases, as well as to the limited number of samples.

Currently, little is known about the biological function of *UBE2G*, and even less about its role in tumors. Previous studies found that *UBE2G* is strongly expressed in the skeletal muscle and participates in the degradation of muscle-specific proteins[44]. Our findings demonstrated that the expression level of *UBE2G* in OC was significantly lower than in normal ovarian tissues, and that this downregulation was associated with poor PFS in OC patients, suggesting a tumor-suppressive role of this protein in OC. This possibility needs to be verified by further experiments.

Although there are few studies on the roles of *UBE2S* and *UBE2V2* in OC, both genes are involved in the occurrence and progression of other tumors. *UBE2S* was reported to be aberrantly expressed in some gynecological tumors, including breast, cervical, and endometrial cancer, and its knockdown inhibits the proliferation of cancer cells and promotes apoptosis[45-47]. *UBE2V2* overexpression seems to be involved in the pathogenesis of gastric cancer, and is significantly associated with poor prognosis in ER-positive/HER2-negative breast cancer[48, 49]. The current study demonstrated that both *UBE2V2* and *UBE2S* were significantly upregulated in OC compared to normal tissues. However, there was no obvious correlation between their expression levels and prognosis.

UBE2T, also known as *FANCT* or *HSPC150*, is essential for *FANCD2* monoubiquitination. It combines with a specific ubiquitin E3 ligase to degrade specific substrates, contributing to DNA repair in the Fanconi anemia pathway and playing a key role in cell proliferation and the maintenance of genomic stability[50]. Recently, *UBE2T* expression has been reported to be significantly upregulated in hepatocellular carcinoma[10], renal cell carcinoma[51], prostate cancer[15], breast cancer, and lung adenocarcinoma[52], and its high expression is associated with poor prognosis in patients. Consistently, after integrating the data on gene expression and prognostic value obtained from different databases, we found that *UBE2T* was significantly overexpressed in OC compared to normal ovarian tissues, and that its high expression was associated with poor prognosis in both OC and serous ovarian cancer.

Various studies have shown that specific genetic alterations are related to cancer prognosis and potential predictors of cancer metastasis[53, 54]. To verify the correlation between alterations in *UBE2* genes and OC, the cBioPortal database was analyzed, revealing an overall rate of genetic alterations ranging from 13.5% to 28.47% in the OC dataset, and a percentage of individual gene alterations ranging from 0.9% to 4%. However, alterations in single *UBE2* genes had no significant impact on OS or DFS, suggesting that these changes did not directly affect OC prognosis.

Since *UBE2T* displayed the greatest correlation with OC among *UBE2* family members, its clinical effects in OC were further investigated. IHC staining and GEO database analysis confirmed that *UBE2T* expression was significantly increased in ovarian epithelial malignant tumors compared to ovarian epithelial borderline tumors, benign tumor, and normal tissues. The expression level of *UBE2T* in FIGO stage III-IV tumors was significantly higher than in FIGO stage I-II tumors, suggesting that *UBE2T* may promote OC progression. In addition, Cox multivariate analysis indicated high *UBE2T* expression as an independent risk factor affecting the prognosis of patients with EOC. Therefore, *UBE2T* is a candidate biomarker for the prediction of OC prognosis.

Multiple evidence indicates that *UBE2T* acts as an oncogene in a variety of tumors, but its molecular mechanism of action varies in different types of cancer. One study showed that *UBE2T* plays a role in the proliferation and invasion of hepatocellular carcinoma cells by regulating the G2/M transition of the cell cycle through the cyclin B1-CDK1 pathway[55], while another study found that *UBE2T* enhances p53 ubiquitination and degradation, promoting the carcinogenesis of hepatocellular carcinoma[10]. Furthermore, *UBE2T* downregulation reduces the activity of the PI3K/Akt signaling pathway, thus inhibiting the proliferation and migration of renal cell carcinoma [51] and osteosarcoma cells[56]. Moreover, *UBE2T* promotes breast cancer progression by directly regulating the BRCA1/BARD1 complex[12]. Furthermore, *UBE2T* promotes nasopharyngeal carcinoma cell proliferation, invasion, and metastasis by activating the AKT/GSK3β/β-catenin pathway[57]. Finally, *UBE2T* silencing in bladder or gastric cancer was found to induce cell cycle arrest in G2/M phase, thereby promoting cancer cell apoptosis and inhibiting tumor growth[13, 14]. However, the role of *UBE2T* in OC has not yet been investigated.

To clarify the role of *UBE2T* in OC at the molecular level, the functions and relevant pathways of *UBE2T* co-expressed genes were investigated by enrichment analysis using the Metascape database. These genes were mainly involved in processes related to cell cycle, including cell division, cell cycle phase transition, DNA replication, and DNA repair, and predominantly implicated in cell cycle regulation, Fanconi anemia signaling, and p53 signaling. GSEA results revealed that patients with high *UBE2C* expression were significantly enriched in E2F_TARGETS and G2M_ CHECKPOINT. KEGG pathway analysis elucidated that the *UBE2T* high expression mutation group was significantly enriched in focal adhesion, calcium signaling, and ECM-receptor interactions. These processes are critical for tumor progression, which could explain the role and molecular function of *UBE2T* in OC.

In patients with high *UBE2T* expression, *TP53*, *TTN*, *DST*, *FAT3*, *CSMD1*, *MUC16*, and *MUC17* exhibited a significant rate of alterations. *TP53* mutation frequency in ovarian serous carcinomas has been reported to range from 50% and 80%[58]; ubiquitous *TP53* mutations are characteristic of high-grade serous ovarian cancer (HGSOC) and related to relapse[59]. *TTN* encodes a large polypeptide expressed in many cancer cell types and involved in oncogenesis, and its mutation has been found in OC by using an the next-generation sequencing (NGS) library[60]. *CSDM1* was present in the genome-wide homozygous deletion profiling of HGSOC[61]. Gene expression profiling showed that *MUC16* and *MUC17* are overexpressed in the majority of serous and mucinous ovarian carcinomas, respectively[62, 63]. We hypothesize that mutations in these genes may be related to the high level of *UBE2T* expression in OC. In addition, gene amplification and hypomethylation were also identified as possible causes of *UBE2T* overexpression.

Growing evidence is being provided that the interaction between immune and cancer cells in the tumor microenvironment has an impact on tumor progression[30]. OC is an immunogenic tumor that can be recognized and attacked by the immune system. The accumulation of TILs in OC microenvironment is related to prolonged OS of the patients, while immune escape events are associated with poor prognosis [64, 65]. In this study, the correlation between *UBE2T* expression and the levels of infiltrating immune cells was analyzed by using the TISIDB-OV database. Particularly strong correlations were found between *UBE2T* expression and the level of specific TIL populations (eosinophils, Act_CD4, neutrophils, and memory B cells), immune inhibitors (*CSF1R*, *TGFB1*, *KDR*, and *CD160*), immune stimulators (*NTSE*, *TNFSF14*, and *TNFSF15*), and MHC molecules (HLA-E, HLA-DOA, HLA-DQA1, and HLA-DQB1). The infiltration of B cells in HGSOC promotes anti-tumor responses, and chemotherapy enhances memory B cell response. Hence, the presence of B cells is a predictor of improved survival in patients with OC[66]. *CSF1R* is overexpressed in OC and the determination of its circulating levels proved useful for disease detection and the evaluation of therapeutic efficacy[67]. It has been reported that the cells of ovarian carcinoma produce large amounts of TGF-β1, which facilitates their escape from the immune system, and the clinical efficacy of immunotherapy based on TGF-β1-silenced tumor vaccines for OC has been investigated[68]. We speculate that *UBE2T* overexpression may cause the reduction or depletion of immune cells, leading to tumor progression by immune escape.

Conclusion

In summary, our bioinformatics analyses highlighted a potential role of *UBE2s* in OC onset and progression. However, our findings need to be supported by additional research and clinical data. IHC and GEO analysis confirmed that *UBE2T* was significantly upregulated in OC, and that its high expression was an independent risk factor and prognostic predictor for OC. *UBE2T* is also a potential biomarker for early diagnosis and a candidate immune-related therapeutic target for OC. However, the biological properties of *UBE2T* and the molecular events related to its overexpression in OC need to be further explored.

Abbreviations

OC: Ovarian cancer; EOC: Epithelial ovarian cancer; GEPIA: The Gene Expression Profiling Interactive Analysis; TCGA: The Cancer Genome Atlas; GTEx: Genotype-tissue Expression dataset projects; GEO: Gene Expression Omnibus; OS:Overall survial; DFS: Disease-free survival; PFS: Progression-free survival; PPI: Protein-protein interaction; GO: Gene Ontology; KEGG: Kyoto Encyclopedia of Genes and Genomes; TILs: Tumor-infiltrating lymphocytes; MHC: Major histocompatibility complex; FIGO: International Federation of Gynecology and Obstetrics; CI: Confidence interval; UBE2: Ubiquitin conjugating enzyme E2; GSEA: Gene set enrichment analysis; CNV: Copy number variation; IHC: Immunohistochemical; HR: Hazard ratio; OCCs: Ovarian cancer cells; HGSOC: High-grade serous ovarian cancer.

Supplementary Information

Additional file 1: Table S1. GO biological process enrichment and KEGG pathway analysis of UBE2s and their interactors.

Additional file 2: Table S2. Related information of UBE2T co-expressed genes.

Declarations

Ethics approval and consent to participate

Ethical approval for this study was obtained from the Clinical Research Ethics Committee of Shengjing Hospital of China Medical University, and all patients provided signed informed consent in accordance with the Declaration of Helsinki.

Consent for publication

All authors have agreed to publish this manuscript

Availability of data and materials

The data generated and/or analysed in this study are available from GEO database (https://www.ncbi.nlm.nih.gov/geo), TCGA (https://portal.gdc.cancer.gov/),

cBioPortal (http://www.cbioportal.org/), and Xena (https://xenabrowser.net/datapages/).

Competing interests

The authors declare that they have no conflict of interest.

Funding

This work was supported by grants from National Natural Science Foundation of China Youth Science Foundation (No. 81602438), Doctoral start-up fund of Liaoning Province (Grant No. 201601133), 345 Talent Project of Shengjing Hospital.

Authors' Contributions

LZ and RZ designed research. RZ and HX wrote manuscript. FL performed the immunohistochemical assay. SW involved in data collection and data statistical analysis. LZ provided fund support and critically reviewed the manuscript. All authors read and approved the final manuscript.

Acknowledgements

None.

Author details

[1]Department of Obstetrics and Gynecology, Shengjing Hospital of China Medical University, Shenyang 110004, Liaoning, China. [2]Key Laboratory of Maternal-Fetal Medicine of Liaoning Province, Key laboratory of Obstetrics and Gynecology of Higher Education of Liaoning Province, Liaoning, China. [3]Department of Gynecology, Shandong Provincial Hospital Affiliated to Shandong First Medical University, Jinan 250021, Shandong, China.

References

1. Siegel RL, Miller KD, Jemal A. Cancer statistics, 2018. CA Cancer J Clin. 2018;68(1):7.
2. Rottmann M, Burges A, Mahner S, Anthuber C, Beck T, Grab D, et al. Cancer of the ovary, fallopian tube, and peritoneum: a population-based comparison of the prognostic factors and outcomes. J Cancer Res Clin Oncol. 2017;143(9):1833-44.
3. Jadidi-Niaragh F, Ghalamfarsa G, Yousefi M, Tabrizi MH, Shokri F. Regulatory T cells in chronic lymphocytic leukemia: implication for immunotherapeutic interventions. Tumour Biol. 2013;34(4):2031-9.
4. Clague MJ, Heride C, Urbé S. The demographics of the ubiquitin system. Trends Cell Biol. 2015;25(7):417-26.
5. Garg P, Ceccarelli DF, Keszei AFA, Kurinov I, Sicheri F, Sidhu SS. Structural and Functional Analysis of Ubiquitin-based Inhibitors That Target the Backsides of E2 Enzymes. J Mol Biol. 2020; 432:952-66.

6. Somasagara RR, Tripathi K, Spencer SM, Clark DW, Barnett R, Bachaboina L, et al. Rad6 upregulation promotes stem cell-like characteristics and platinum resistance in ovarian cancer. Biochem Biophys Res Commun. 2016;469(3):449-55.
7. Matsumoto A, Ishibashi Y, Urashima M, Omura N, Nakada K, Nishikawa K, et al. High UBCH10 protein expression as a marker of poor prognosis in esophageal squamous cell carcinoma. Anticancer Res. 2014;34(2):955-61.
8. Zhou W, Xu J, Li H, Xu M, Chen ZJ, Wei W, et al. Neddylation E2 UBE2F Promotes the Survival of Lung Cancer Cells by Activating CRL5 to Degrade NOXA via the K11 Linkage. Clin Cancer Res. 2017;23(4):1104-16.
9. Machida YJ, Machida Y, Chen Y, Gurtan AM, Kupfer GM, D'Andrea AD, et al. UBE2T is the E2 in the Fanconi anemia pathway and undergoes negative autoregulation. Mol Cell. 2006;23(4):589-96.
10. Liu LP, Yang M, Peng QZ, Li MY, Zhang YS, Guo YH, et al. UBE2T promotes hepatocellular carcinoma cell growth via ubiquitination of p53. Biochem Biophys Res Commun. 2017;493(1):20-27.
11. Hao J, Xu A, Xie X, Hao J, Tian T, Gao S, et al. Elevated expression of UBE2T in lung cancer tumors and cell lines. Tumour Biol. 2008;29(3):195-203.
12. Ueki T, Park JH, Nishidate T, Kijima K, Hirata K, Nakamura Y, et al. Ubiquitination and downregulation of BRCA1 by ubiquitin-conjugating enzyme E2T overexpression in human breast cancer cells. Cancer Res. 2009;69(22):8752-60.
13. Luo C, Yao Y, Yu Z, Zhou H, Guo L, Zhang J, et al. UBE2T knockdown inhibits gastric cancer progression. Oncotarget. 2017;8(20): 32639-54.
14. Gong YQ, Peng D, Ning XH, Yang XY, Li XS, Zhou LQ, et al. UBE2T silencing suppresses proliferation and induces cell cycle arrest and apoptosis in bladder cancer cells. Oncol Lett. 2016;12(6):4485-92.
15. Wen M, Kwon Y, Wang Y, Mao JH, Wei G. Elevated expression of UBE2T exhibits oncogenic properties in human prostate cancer. Oncotarget. 2015;6(28):25226-39.
16. Rhodes DR, Yu J, Shanker K, Deshpande N, Varambally R, Ghosh D, et al. ONCOMINE: a cancer microarray database and integrated data-mining platform. Neoplasia. 2004;6(1):1-6.
17. Tang Z, Li C, Kang B, Gao G, Li C, Zhang Z. GEPIA: a web server for cancer and normal gene expression profiling and interactive analyses. Nucleic Acids Res. 2017;45:W98-W102.
18. Karlan BY, Dering J, Walsh C, Orsulic S, Lester J, Anderson LA, et al. POSTN/TGFBI-associated stromal signature predicts poor prognosis in serous epithelial ovarian cancer. Gynecol Oncol. 2014;132(2):334-42.
19. Winterhoff B, Hamidi H, Wang C, Kalli KR, Fridley BL, Dering J, et al. Molecular classification of high grade endometrioid and clear cell ovarian cancer using TCGA gene expression signatures. Gynecol Oncol. 2016;141(1):95-100.
20. Lisowska KM, Olbryt M, Student S, Kujawa KA, Cortez AJ, Simek K, et al. Unsupervised analysis reveals two molecular subgroups of serous ovarian cancer with distinct gene expression profiles and survival. J Cancer Res Clin Oncol. 2016;142(6):1239-52.

21. Gyorffy B, Lánczky A, Szállási Z. Implementing an online tool for genome-wide validation of survival-associated biomarkers in ovarian-cancer using microarray data from 1287 patients. Endocr Relat Cancer. 2012;19(2):197-208.
22. Szklarczyk D, Morris JH, Cook H, Kuhn M, Wyder S, Simonovic M, et al. The STRING database in 2017: quality-controlled protein-protein association networks, made broadly accessible. Nucleic Acids Res. 2017;45:D362-8.
23. Zhou Y, Zhou B, Pache L, Chang M, Khodabakhshi AH, Tanaseichuk O, et al. Metascape provides a biologist-oriented resource for the analysis of systems-level datasets. Nat Commun. 2019;10(1):1523.
24. Ru B, Wong CN, Tong Y, Zhong JY, Zhong SSW, Wu WC, et al. TISIDB: an integrated repository portal for tumor-immune system interactions. Bioinformatics. 2019;35(20):4200-02.
25. Yoshihara K, Tajima A, Komata D, Yamamoto T, Kodama S, Fujiwara H, et al. Gene expression profiling of advanced-stage serous ovarian cancers distinguishes novel subclasses and implicates ZEB2 in tumor progression and prognosis. Cancer Sci. 2009;100(8):1421-8.
26. Lu KH, Patterson AP, Wang L, Marquez RT, Atkinson EN, Baggerly KA, et al. Selection of potential markers for epithelial ovarian cancer with gene expression arrays and recursive descent partition analysis. Clin Cancer Res. 2004;10(10):3291-300.
27. Adib TR, Henderson S, Perrett C, Hewitt D, Bourmpoulia D, Ledermann J, et al. Predicting biomarkers for ovarian cancer using gene-expression microarrays. Br J Cancer. 2004;90(3):686-92.
28. Welsh JB, Zarrinkar PP, Sapinoso LM, Kern SG, Behling CA, Monk BJ, et al. Analysis of gene expression profiles in normal and neoplastic ovarian tissue samples identifies candidate molecular markers of epithelial ovarian cancer. Proc Natl Acad Sci USA. 2001;98(3):1176-81.
29. Bonome T, Levine DA, Shih J, Randonovich M, Pise-Masison CA, Bogomolniy F, et al. A gene signature predicting for survival in suboptimally debulked patients with ovarian cancer. Cancer Res. 2008;68(13):5478-86.
30. Hosseini SM, Okoye I, Chaleshtari MG, Hazhirkarzar B, Mohamadnejad J, Azizi G, et al. E2 ubiquitin-conjugating enzymes in cancer: Implications for immunotherapeutic interventions. Clin Chim Acta. 2019;498:126-34.
31. Koken MH, Reynolds P, Jaspers-Dekker I, Prakash L, Prakash S, Bootsma D, et al. Structural and functional conservation of two human homologs of the yeast DNA repair gene RAD6. Proc Natl Acad Sci USA. 1991;88(20):8865-9.
32. Somasagara RR, Spencer SM, Tripathi K, Clark DW, Mani C, Madeira da Silva L, et al. RAD6 promotes DNA repair and stem cell signaling in ovarian cancer and is a promising therapeutic target to prevent and treat acquired chemoresistance. Oncogene. 2017;36(48):6680-90.
33. Zhang J, Liu X, Yu G, Liu L, Wang J, Chen X, et al. UBE2C Is a Potential Biomarker of Intestinal-Type Gastric Cancer With Chromosomal Instability. Front Pharmacol. 2018; 9: 847.
34. Gong Y, Wang D, Lin L, Dai J, Yu L. The expression of ubiquitin-conjugating enzyme E2C and KAI1 in ovarian carcinoma and their clinical significance. Medicine (Baltimore). 2019;98(46):e17896.

35. Berlingieri MT, Pallante P, Guida M, Nappi C, Masciullo V, Scambia G, et al. UbcH10 expression may be a useful tool in the prognosis of ovarian carcinomas. Oncogene. 2007;26(14):2136-40.
36. Hong X, Li S, Li W, Xie M, Wei Z, Guo H, et al. Disruption of protein neddylation with MLN4924 attenuates paclitaxel-induced apoptosis and microtubule polymerization in ovarian cancer cells. Biochem Biophys Res Commun. 2019;508(3):986-90.
37. Zhang M, Windheim M, Roe SM, Peggie M, Cohen P, Prodromou C, et al. Chaperoned ubiquitylation–crystal structures of the CHIP U box E3 ubiquitin ligase and a CHIP-Ubc13-Uev1a complex. Mol Cell. 2005;20(4):525-38.
38. Jackson SP, Durocher D. Regulation of DNA damage responses by ubiquitin and SUMO. Mol Cell. 2013;49(5):795-807.
39. Zhu H, Yu JJ. Gene expression patterns in the histopathological classification of epithelial ovarian cancer. Exp Ther Med. 2010;1(1):187-92.
40. Guo Y, Fu P, Zhu H, Reed E, Remick SC, Petros W, et al. Correlations among ERCC1, XPB, UBE2I, EGF, TAL2 and ILF3 revealed by gene signatures of histological subtypes of patients with epithelial ovarian cancer. Oncol Rep. 2012;27(1):286-92.
41. Zhang X, Feng Y, Wang XY, Zhang YN, Yuan CN, Zhang SF, et al. The inhibition of UBC13 expression and blockage of the DNMT1-CHFR-Aurora A pathway contribute to paclitaxel resistance in ovarian cancer. Cell Death Dis. 2018;9(2):93.
42. Xu W, Hu GQ, Da Costa C, Tang JH, Li QR, Du L, et al. Long noncoding RNA UBE2R2-AS1 promotes glioma cell apoptosis via targeting the miR-877-3p/TLR4 axis. Onco Targets Ther. 2019;12:3467-80.
43. Zhang L, Jin Y, Yang H, Li Y, Wang C, Shi Y, et al. SMYD3 promotes epithelial ovarian cancer metastasis by down-regulating p53 protein stability and promoting p53 ubiquitination. Carcinogenesis. 2019;40:1492-503.
44. Watanabe TK, Kawai A, Fujiwara T, Maekawa H, Hirai Y, Nakamura Y, et al. Molecular cloning of UBE2G, encoding a human skeletal muscle-specific ubiquitin-conjugating enzyme homologous to UBC7 of C. elegans. Cytogenet Cell Genet. 1996;74:146-8.
45. Ayesha AK, Hyodo T, Asano E, Sato N, Mansour MA, Ito S, et al. UBE2S is associated with malignant characteristics of breast cancer cells. Tumour Biol. 2016;37(1):763-72.
46. Lin TH, Hsu WH, Tsai PH, Huang YT, Lin CW, Chen KC, et al. Dietary flavonoids, luteolin and quercetin, inhibit invasion of cervical cancer by reduction of UBE2S through epithelial-mesenchymal transition signaling. Food Funct. 2017;8(4):1558-68.
47. Lin M, Lei T, Zheng J, Chen S, Du L, Xie H. UBE2S mediates tumor progression via SOX6/β-Catenin signaling in endometrial cancer. Int J Biochem Cell Biol. 2019;109:17-22.
48. Cheng L, Wang P, Yang S, Yang Y, Zhang Q, Zhang W, et al. Identification of genes with a correlation between copy number and expression in gastric cancer. BMC Med Genomics. 2012;5:14.
49. Santarpia L, Iwamoto T, Di Leo A, Hayashi N, Bottai G, Stampfer M, et al. DNA Repair Gene Patterns as Prognostic and Predictive Factors in Molecular Breast Cancer Subtypes. Oncologist. 2013;18(10):1063-73.

50. Alpi AF, Chaugule V, Walden H. Mechanism and disease association of E2-conjugating enzymes: lessons from UBE2T and UBE2L3. Biochem J. 2016;473(20): 401-19.
51. Hao P, Kang B, Li Y, Hao W, Ma F. UBE2T promotes proliferation and regulates PI3K/Akt signaling in renal cell carcinoma. Mol Med Rep. 2019;20(2):1212-20.
52. Perez-Peña J, Corrales-Sánchez V, Amir E, Pandiella A, Ocana A. Ubiquitin-conjugating enzyme E2T (UBE2T) and denticleless protein homolog (DTL) are linked to poor outcome in breast and lung cancers. Sci Rep. 2017;7(1):17530.
53. Hieronymus H, Murali R, Tin A, Yadav K, Abida W, Moller H, et al. Tumor copy number alteration burden is a pan-cancer prognostic factor associated with recurrence and death. Elife. 2018;7.
54. Pearlman A, Upadhyay K, Cole K, Loke J, Sun K, Fineberg S, et al. Robust genomic copy number predictor of pan cancer metastasis. Genes Cancer. 2018;9:66-77.
55. Liu LL, Zhu JM, Yu XN, Zhu HR, Shi X, Bilegsaikhan E, et al. UBE2T promotes proliferation via G2/M checkpoint in hepatocellular carcinoma. Cancer Manag Res. 2019;11:8359-70.
56. Wang Y, Leng H, Chen H, Wang L, Jiang N, Huo X, et al. Knockdown of UBE2T Inhibits Osteosarcoma Cell Proliferation, Migration, and Invasion by Suppressing the PI3K/Akt Signaling Pathway. Oncol Res. 2016;24(5):361-9.
57. Hu W, Xiao L, Cao C, Hua S, Wu D. UBE2T promotes nasopharyngeal carcinoma cell proliferation, invasion, and metastasis by activating the AKT/GSK3β/β-catenin pathway. Oncotarget. 2016;7(12):15161-72.
58. Salani R, Kurman RJ, Giuntoli R, Gardner G, Bristow R, Wang TL, et al. Assessment of TP53 mutation using purified tissue samples of ovarian serous carcinomas reveals a higher mutation rate than previously reported and does not correlate with drug resistance. Int J Gynecol Cancer. 2008;18(3):487-91.
59. Nelson L, Tighe A, Golder A, Littler S, Bakker B, Moralli D, et al. living biobank of ovarian cancer ex vivo models reveals profound mitotic heterogeneity. Nat Commun. 2020;11(1):822.
60. Zhang L, Luo M, Yang H, Zhu S, Cheng X, Qing C. Next-generation sequencing-based genomic profiling analysis reveals novel mutations for clinical diagnosis in Chinese primary epithelial ovarian cancer patients. J Ovarian Res. 2019;12(1):19.
61. Kuo KT, Guan B, Feng Y, Mao TL, Chen X, Jinawath N, et al. Analysis of DNA Copy Number Alterations in Ovarian Serous Tumors Identifies New Molecular Genetic Changes in Low-Grade and High-Grade Carcinomas. Cancer Res. 2009;69(9):4036-42.
62. Comamala M, Pinard M, Thériault C, Matte I, Albert A, Boivin M, et al. Downregulation of cell surface CA125/MUC16 induces epithelial-to-mesenchymal transition and restores EGFR signalling in NIH:OVCAR3 ovarian carcinoma cells. Br J Cancer. 2011;104(6):989-99.
63. Yang CW, Chang CY, Lai MT, Chang HW, Lu CC, Chen Y, et al. Genetic variations of MUC17 are associated with endometriosis development and related infertility. BMC Med. Genet. 2015;16:60.
64. Yang S, Yin X, Yue Y, Wang S. Application Of Adoptive Immunotherapy In Ovarian Cancer. Onco Targets Ther. 2019;12:7975-91.

65. Ghisoni E, Imbimbo M, Zimmermann S, Valabrega G. Ovarian Cancer Immunotherapy: Turning up the Heat. Int J Mol Sci. 2019;20(12).
66. Gupta P, Chen C, Chaluvally-Raghavan P, Pradeep S. B Cells as an Immune-Regulatory Signature in Ovarian Cancer. Cancers (Basel). 2019;11(7).
67. Farag AK, Hassan AHE, Ahn BS, Park KD, Roh EJ. Reprofiling of pyrimidine-based DAPK1/CSF1R dual inhibitors: identification of 2,5-diamino-4-pyrimidinol derivatives as novel potential anticancer lead compounds. J Enzyme Inhib Med Chem. 2020;35(1):311-24.
68. Wei H, Liu P, Swisher E, Yip YY, Tse JH, Agnew K, et al. Silencing of the TGF-β1 gene increases the immunogenicity of cells from human ovarian carcinoma. J Immunother. 2012;35(3):267-75.

Figures

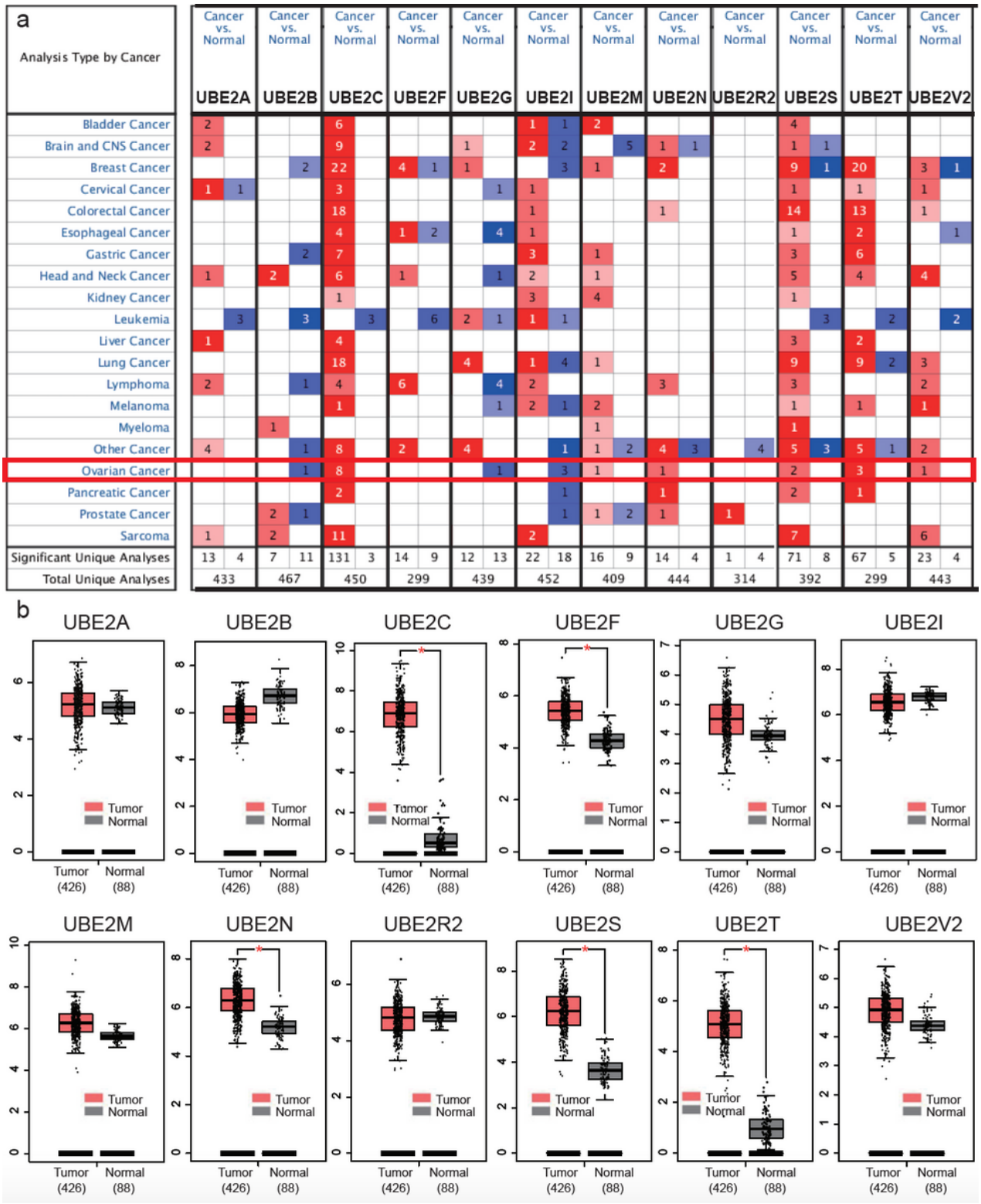

Figure 1

Differential expression of UBE2s in cancer. a The mRNA expression levels of different UBE2 members in various types of cancers (Oncomine). The numbers in the cells represent the data sets meeting the threshold. Red and blue cells represent upregulation and downregulation, respectively. The color intensity reflects the level of significance. b The mRNA levels of UBE2 members in OC and normal ovarian tissues

(GEPIA). The box plots indicate UBE2 expression in 426 cases of OC (red) and 88 cases of corresponding normal tissues (gray). *P<0.01

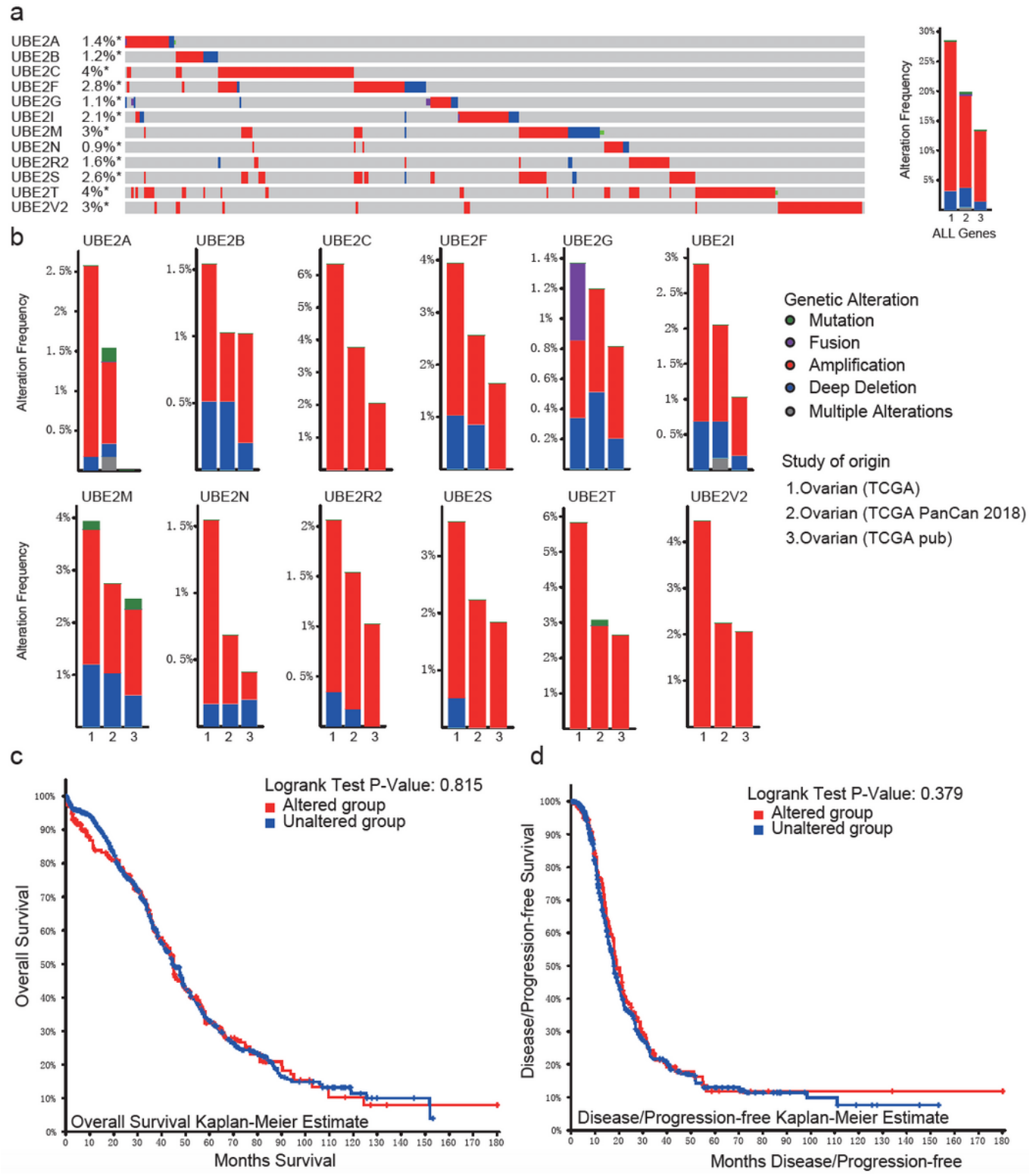

Figure 2

Frequency of UBE2 gene alterations in OC (cBioPortal). a Left, OncoPrint visual summary of alterations in UBE2 family members; right, summary of genetic alteration frequency in UBE2 genes. b Analysis of genetic alteration frequency in UBE2 family members in three datasets (TCGA, TCGA PanCan, and TCGA

pub). The alterations included amplification (red), mutations (green), fusions (purple), deep deletions (blue), and multiple alterations (grey). c Kaplan-Meier plots comparing OS in cases with and without UBE2 gene alterations. d Kaplan-Meier plots comparing DFS in cases with and without UBE2 gene alterations

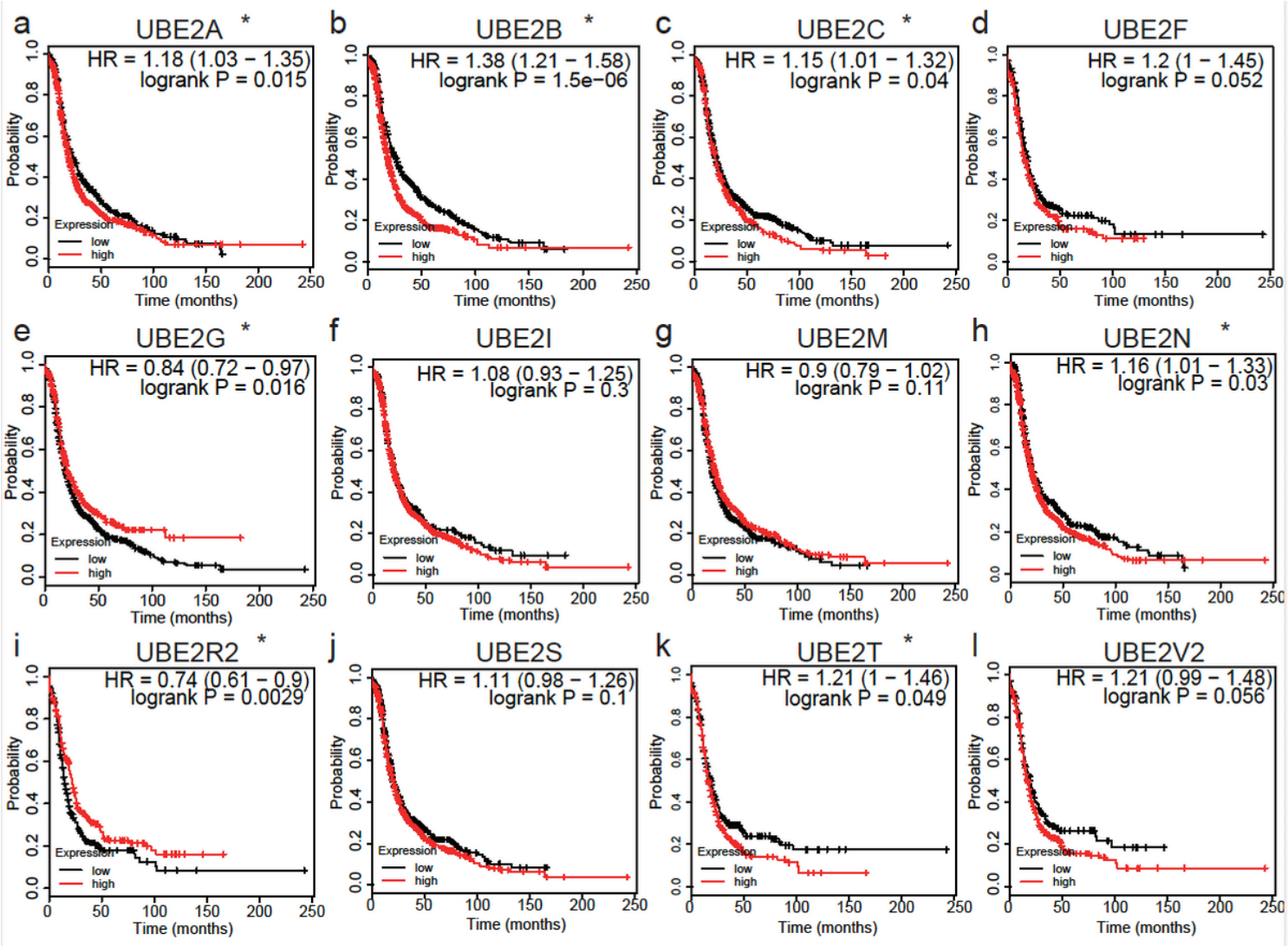

Figure 3

Prognostic value of UBE2 mRNA levels in patients with OC (PFS in Kaplan-Meier plotter). . a-l Prognostic significance of individual UBE2 members in OC. Red line means high expression and black line means low expression. The P values were calculated using the log-rank test. *P<0.05

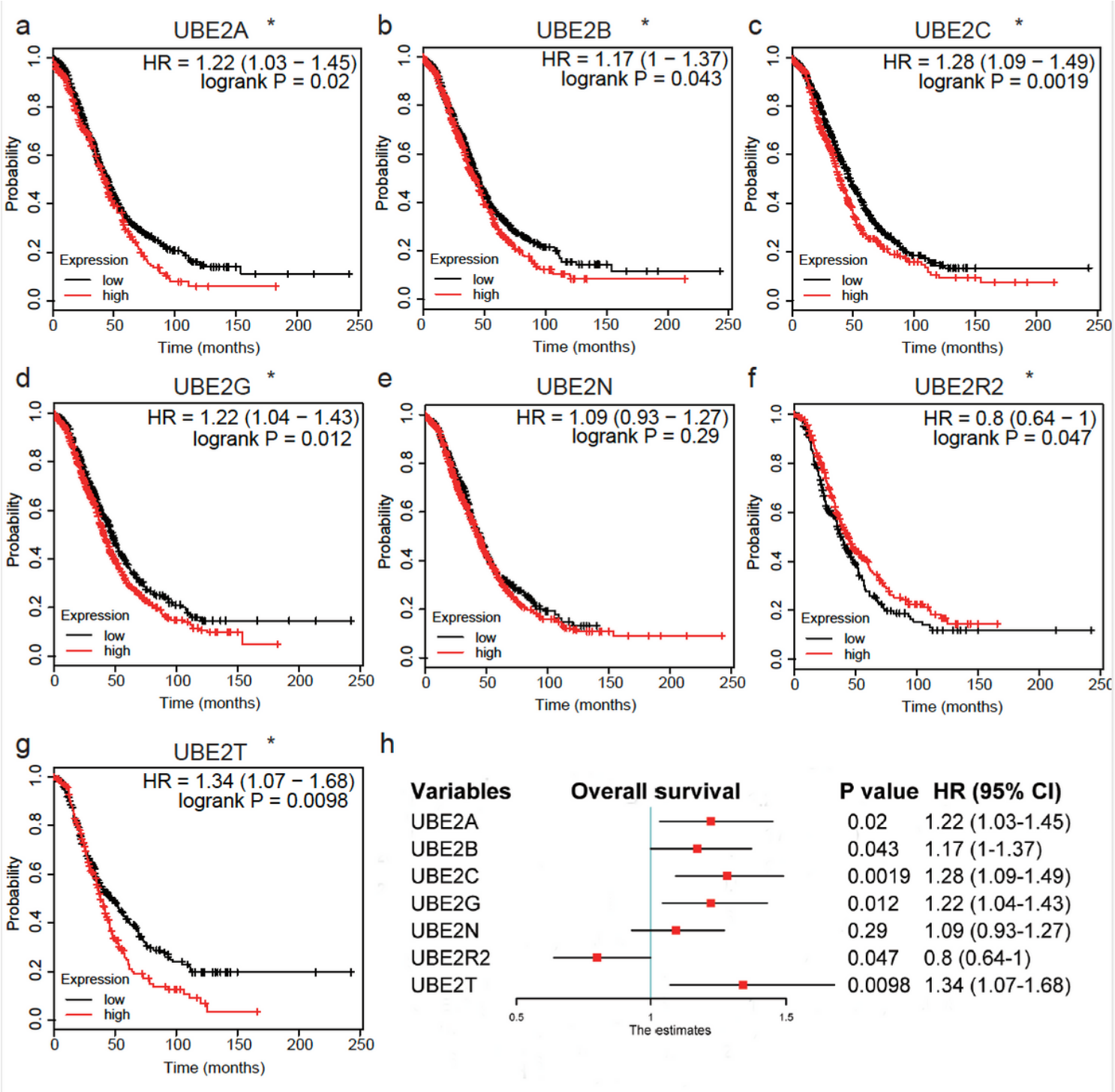

Figure 4

Prognostic value of UBE2 mRNA levels in patients with ovarian serous tumors (OS in Kaplan-Meier plotter). a-g Prognostic significance of individual UBE2s in ovarian serous tumors. h Prognostic HRs of individual UBE2s in ovarian serous tumors. Red line means high expression and black line means low expression. The P values were calculated using the log-rank test. *P<0.05

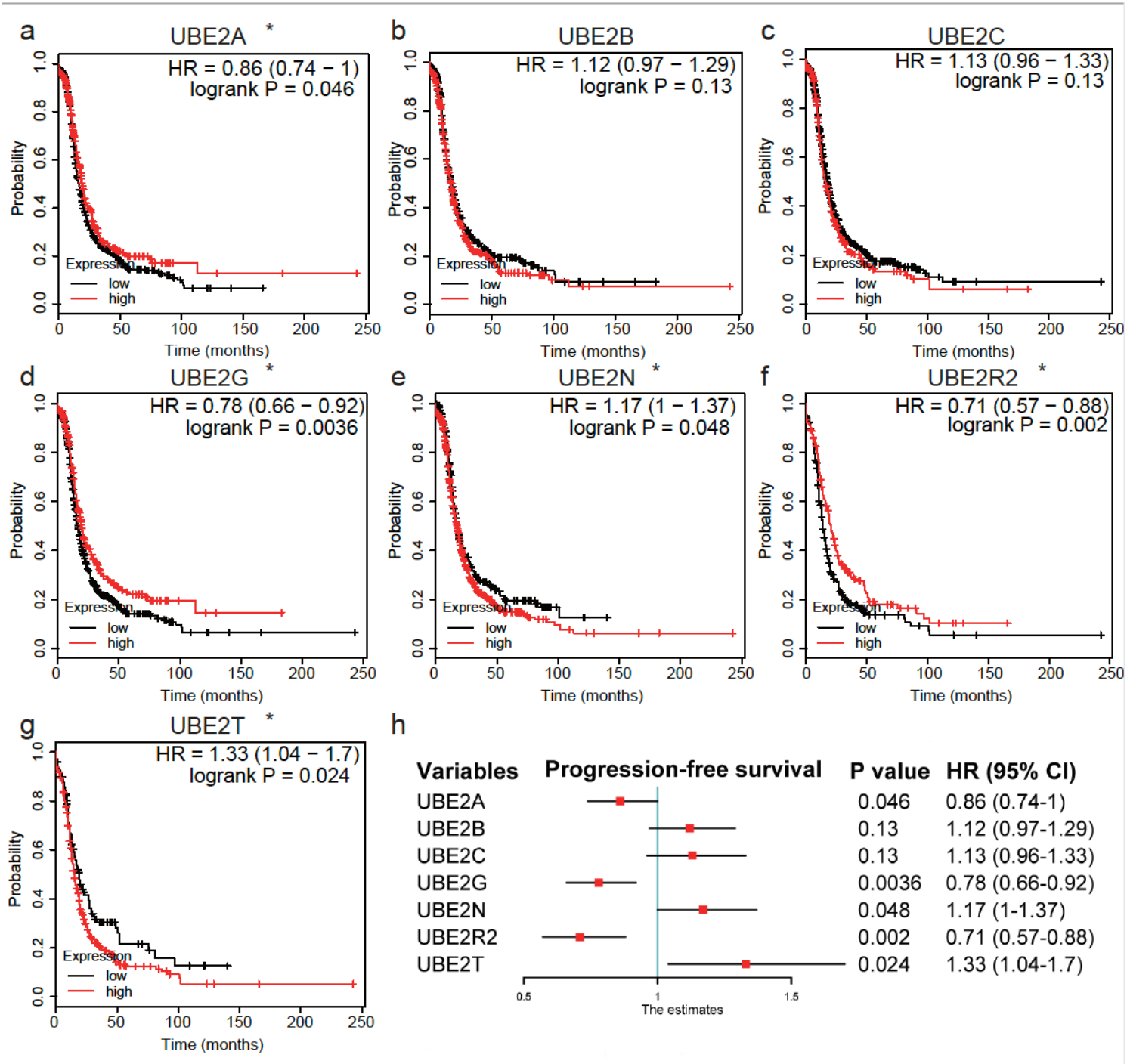

Figure 5

Prognostic value of UBE2 mRNA levels in patients with ovarian serous tumors (PFS in Kaplan-Meier plotter). a-g Prognostic significance of individual UBE2s in ovarian serous tumors. h Prognostic HRs of individual UBE2s in ovarian serous tumors. Red line means high expression and black line means low expression. The P values were calculated using the log-rank test. *P<0.05

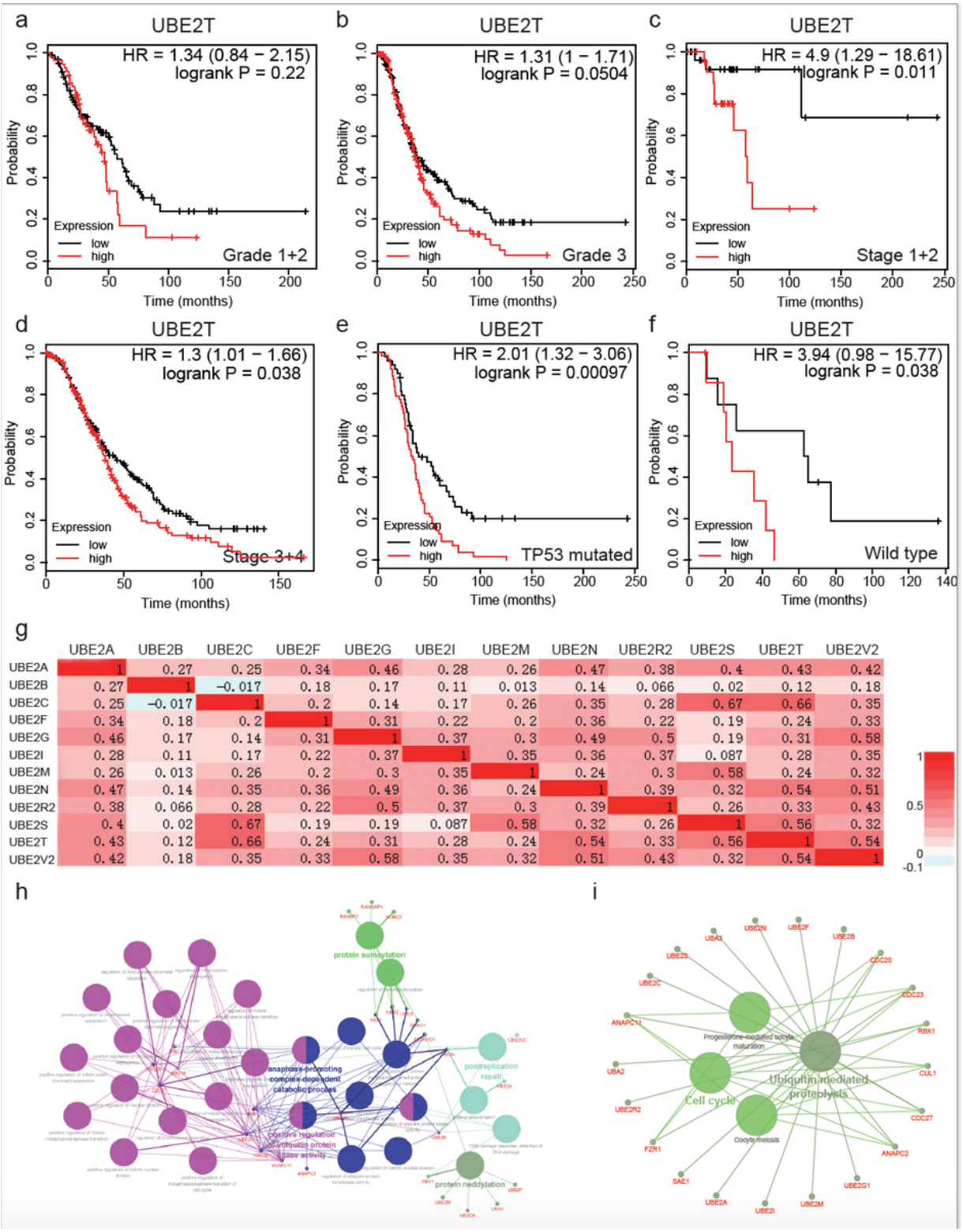

Figure 6

Prognostic significance of UBE2T expression level in ovarian serous tumors of different pathological grade (a,b), FIGO stage (c,d), and TP53 mutational status (e,f) (OS in Kaplan-Meier plotter). Analysis of the interactions between UBE2 family members (GEPIA and Cytoscape). g Spearman' s correlation coefficients between UBE2 family members. Red and blue cells represent positive and negative correlations, respectively. The color intensity reflects the strength of the correlations. h GO biological

process enrichment analysis of UBE2s and their interactors. i KEGG pathway analysis of UBE2s and their interactors. *P<0.05

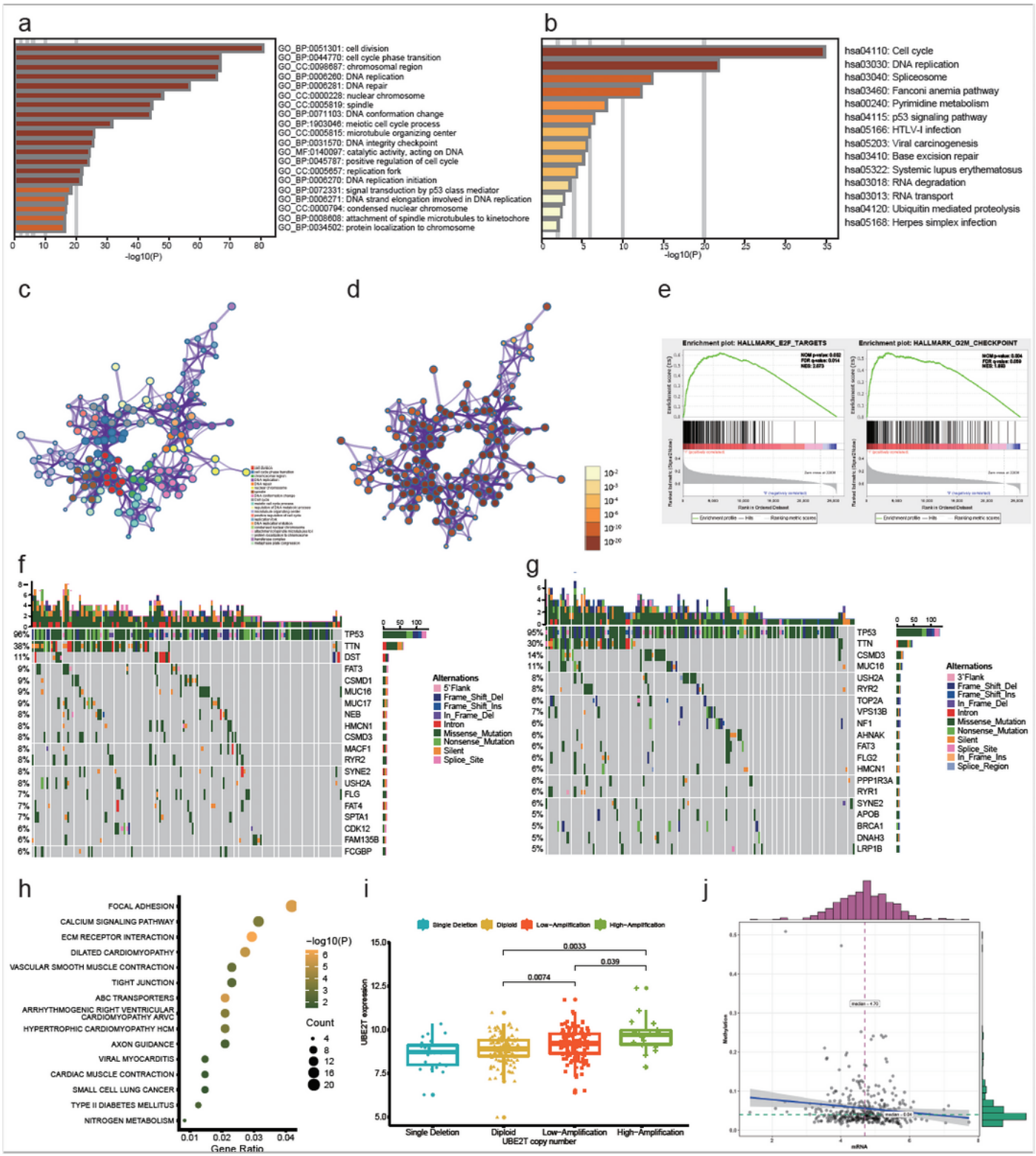

Figure 7

Molecular mechanisms related to UBE2T expression in ovarian cancer (Metascape). a Bar graph of GO enriched terms colored by P-values. b Bar graph of KEGG enriched terms colored by P-values. c Network of enriched terms colored according to clusters: terms belonging to the same cluster are more closely

related to each other. d Network of enriched terms colored according to P-value: the higher the number of genes in each term, the higher the statistical significance. e Gene sets significantly enriched in patients with high UBE2T expression (HALLMARK_E2F_TARGETS and HALLMARK_G2M_ CHECKPOINT). f Top 20 somatically mutated genes in patients with high UBE2T expression. g Top 20 somatically mutated genes in patients with low UBE2T expression. h KEGG pathway analysis in the UBE2T high expression mutation group. i Analysis of the correlation between copy number variation and UBE2T expression. j Analysis of the correlation between methylation and UBE2T expression

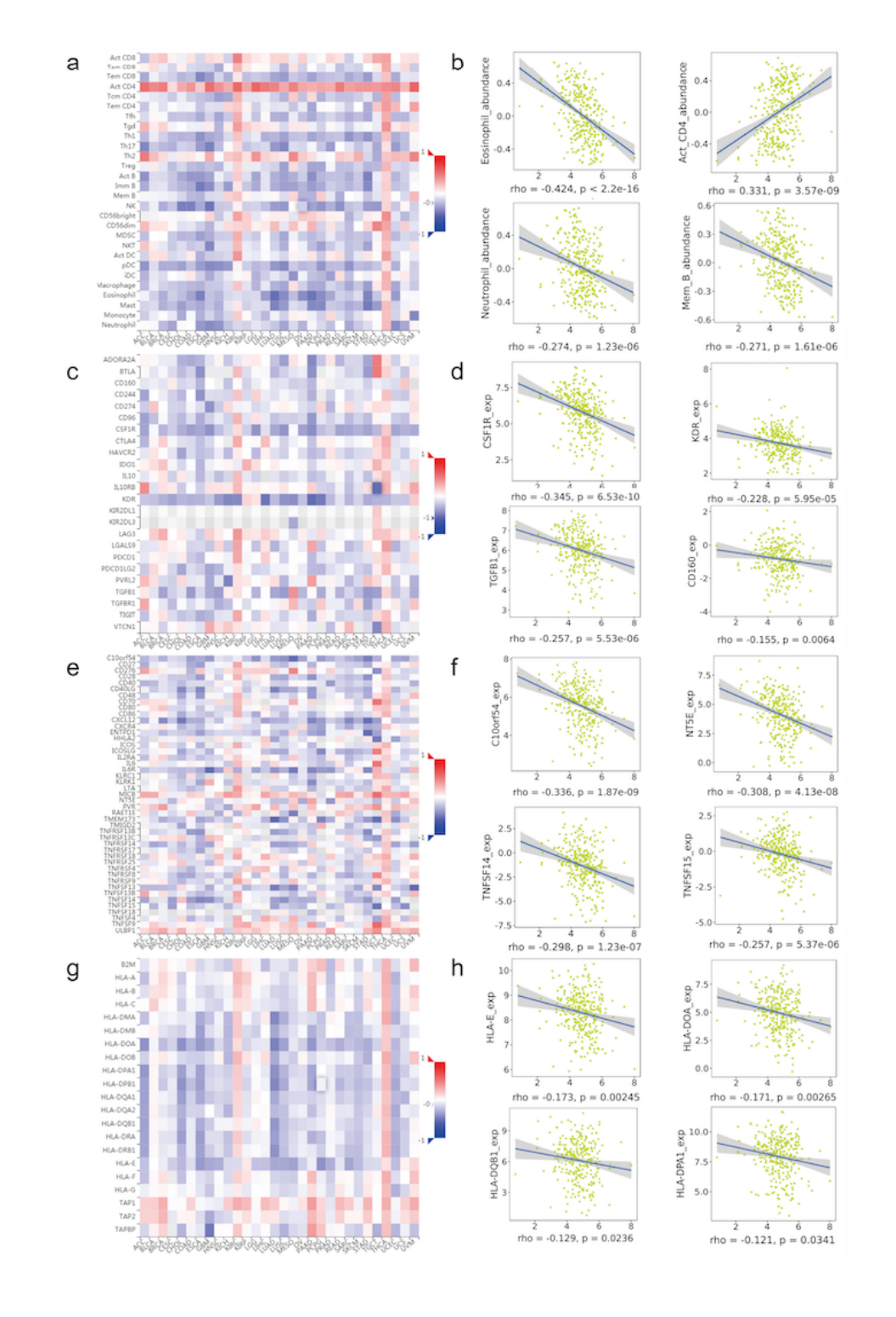

Figure 8

The correlation between immune factors and UBE2T in ovarian cancer determined by TISIDB analysis. a Correlation between UBE2T expression and tumor-infiltrating lymphocytes (TILs). b TILs with the highest correlation with UBE2T expression. c Correlation between UBE2T expression and immune inhibitors. d Immune inhibitors showing the highest correlation with UBE2T expression. e Correlation between UBE2T expression and immune stimulators. f Immune stimulators showing the highest correlation with UBE2T expression. g Correlation between UBE2T expression and MHC molecules. h MHC molecules exhibiting the highest correlation with UBE2T expression. Red and blue cells indicate positive and negative correlations, respectively. The color intensity reflects the strength of the correlation.

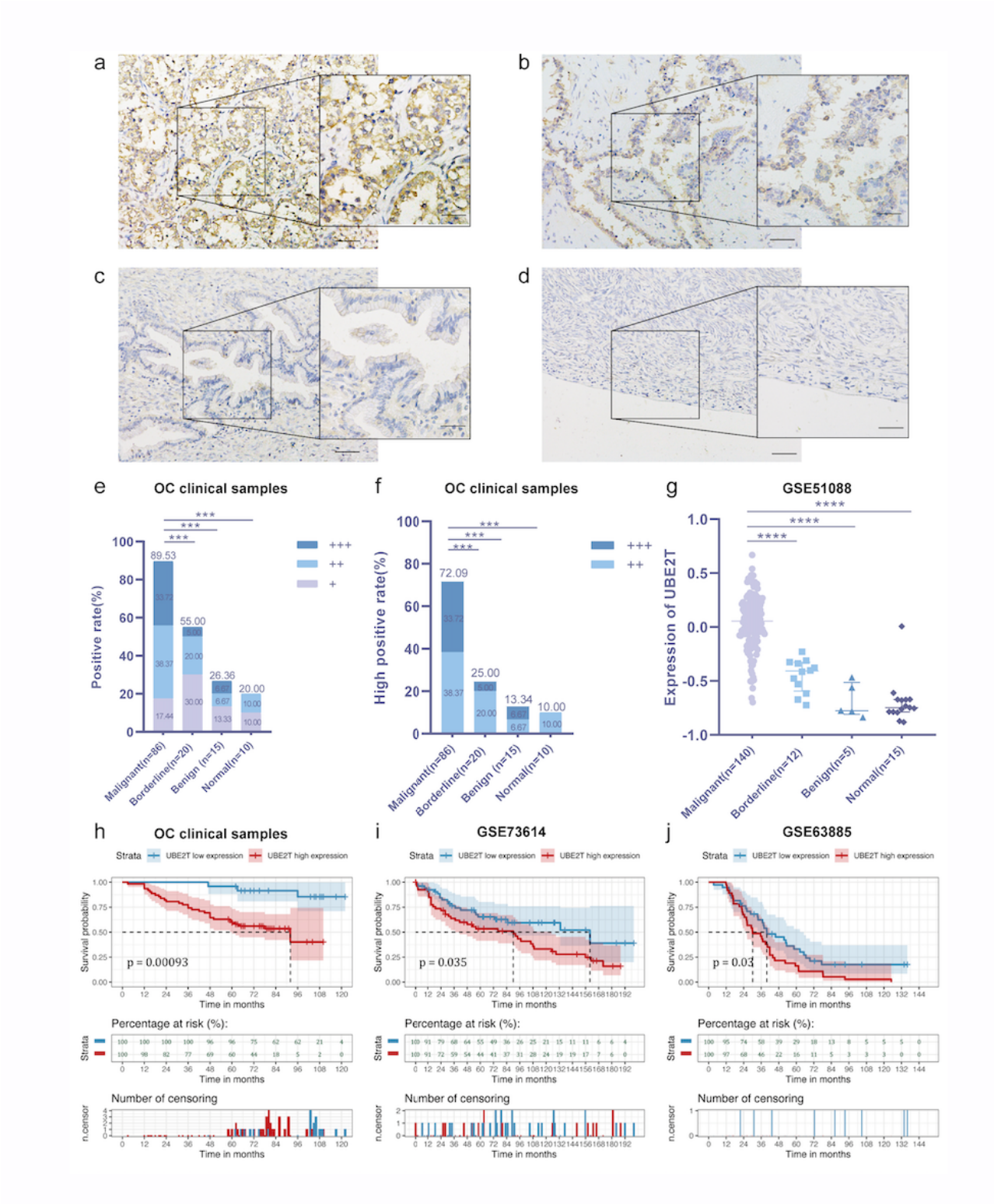

Figure 9

UBE2T expression in different ovarian tissues. Immunohistochemical detection of UBE2T in OC tissues (a), borderline tumors (b), benign tumors (c), and normal ovarian tissues (d) (magnification, left ×200, right ×400). e Positive rates of UBE2T expression in clinical samples of different groups. f Highly positive rates of UBE2T expression in clinical samples of different groups. g UBE2T expression in the different groups, according to the GSE51088 dataset. h Correlation between UBE2T expression and overall survival

in 86 patients, based on clinical samples. i Correlation between UBE2T expression and overall survival in 107 samples, according to the GSE73614 dataset. j Correlation between UBE2T expression and overall survival in 75 samples, according to the GSE63885 dataset. *P<0.05, **P<0.01, ***P<0.001, **** P<0.0001

Supplementary Files

This is a list of supplementary files associated with this preprint. Click to download.

- Additionalfile1.xls
- Additionalfile2.xlsx